AD-760 131

LASER-INDUCED DAMAGE IN OPTICAL MATERIALS

Concetto R. Giuliano

Hughes Research Laboratories

Prepared for:

Air Force Cambridge Research Laboratories
Defense Advanced Research Projects Agency

January 1973

AFCRL-TR-73-0099

17

LASER-INDUCED DAMAGE IN OPTICAL MATERIALS

By
CONCETTO R. GIULIANO

HUGHES RESEARCH LABORATORIES
3011 MALIBU CANYON ROAD
MALIBU, CALIFORNIA 90265

CONTRACT F19628-72-C-0348
PROJECT 2042
SEMIANNUAL TECHNICAL REPORT

JANUARY 1973

CONTRACT MONITOR: HAROLD POSEN
SOLID STATE SCIENCES LABORATORY

APPROVED FOR PUBLIC RELEASE; DISTRIBUTION UNLIMITED.

Sponsored by
DEFENSE ADVANCED RESEARCH PROJECTS AGENCY
ARPA ORDER 2042

Monitored by
AIR FORCE CAMBRIDGE RESEARCH LABORATORIES
AIR FORCE SYSTEMS COMMAND
UNITED STATES AIR FORCE
BEDFORD, MASSACHUSETTS 01730

60

ARPA Order No. 2042

Program Code No. 3D10

Contractor: Hughes Research Laboratories

Effective Date of Contract: 15 June 1972

Contract No. F19628-72-C-0348

Principal Investigator and Phone No.
Dr. Concetto R. Giuliano/213
456-6411 Ext. 437

AFCRL Project Scientist and Phone No.
Dr. Harold Posen/615 861-3532

Contract Expiration Date:
15 December 1973

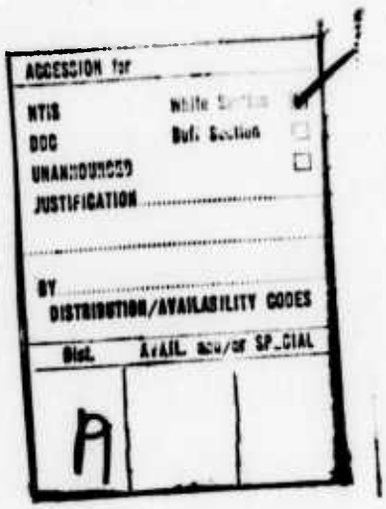

Qualified requestors may obtain additional copies from the Defense Documentation Center. All others should apply to the National Technical Information Service.

UNCLASSIFIED

Security Classification

DOCUMENT CONTROL DATA - R&D

(Security classification of title, body of abstract and indexing annotation must be entered when the overall report is classified)

1. ORIGINATING ACTIVITY *(Corporate author)*
Hughes Research Laboratories
3011 Malibu Canyon Road
Malibu, California 90265

2a. REPORT SECURITY CLASSIFICATION
Unclassified

2b. GROUP
N/A

3. REPORT TITLE

LASER-INDUCED DAMAGE IN OPTICAL MATERIALS

4. DESCRIPTIVE NOTES *(Type of report and inclusive dates)*
Scientific. Interim.

5. AUTHOR(S) *(First name, middle initial, last name)*

Concetto R. Giuliano

6. REPORT DATE	7a. TOTAL NO. OF PAGES	7b. NO. OF REFS
January 1973	~~56~~ 60	20

8a. CONTRACT OR GRANT NO.	9a. ORIGINATOR'S REPORT NUMBER(S)
F19628-72-C-0348, ARPA Order No. 2042 b. PROJECT, TASK, WORK UNIT NOS. 2042 N/A N/A c. DOD ELEMENT 62701E d. DOD SUBELEMENT N/A	9b. OTHER REPORT NO(S) *(Any other numbers that may be assigned this report)* AFCRL-TR-73-0049

10. DISTRIBUTION STATEMENT

11. SUPPLEMENTARY NOTES	12. SPONSORING MILITARY ACTIVITY
This research was supported by the Defense Advanced Research Projects Agency.	Air Force Cambridge Research Labs. Air Force Systems Command, U.S. AF L.G. Hanscom Field Bedford, Massachusetts 01730

13. ABSTRACT This report describes the results of surface damage experiments performed at 1.06 μm on proustite (Ag_3AsS_3) and at 0.694 μm on sapphire (α-Al_2O_3). A discussion of surface damage morphology of proustite for cw and pulsed illumination is illustrated using optical and scanning electron micrographs. The morphology of surface damage close to threshold suggests that the mechanism involves the absorption of laser radiation by small absorbing centers, possibly inclusions or surface impurities. Damage thresholds for proustite are presented for pulses of different durations at 1.06 μm (18 nsec and ~260 nsec) and the results are discussed in the context of a thermal mechanism. Damage thresholds of low-reflectivity sputtered alumina films on proustite were compared with thresholds for an uncoated surface of the same sample, and an appreciable increase in threshold (~40%) was observed in some cases indicating the feasibility of providing a protective film for proustite. A series of damage threshold studies on ion beam polished sapphire was performed as a continuation of work performed on an earlier program. A threshold increase of up to ten times was observed, but a large scatter in the data is evident. The total energy and temporal pulse shape of transmitted pulses at 0.694 μm have been compared with incident pulses as a function of incident power from sapphire surface damage threshold to many times higher. Results of experiments of this type are described for different focusing conditions and for different angles of incidence in air and in vacuum. A close connection with the dynamics of breakdown is evident in these data, but a detailed interpretation is not offered.

DD FORM 1 NOV 65 1473

UNCLASSIFIED

Security Classification

14. KEY WORDS	LINK A		LINK B		LINK C	
	ROLE	WT	ROLE	WT	ROLE	WT
Laser Damage						
Proustite						
Sapphire						
0.694 and 1.06 μm						
Pulse Duration Dependence						
Ion Beam Polishing						
Single Mode Lasers						
Surface Damage						

AFCRL-TR-73-0099

LASER-INDUCED DAMAGE IN OPTICAL MATERIALS

by

Concetto R. Giuliano

HUGHES RESEARCH LABORATORIES
3011 Malibu Canyon Road
Malibu, California 90265

Contract F19628-72-C-0348

Project 2042

Semiannual Technical Report
January 1973

Contract Monitor: Harold Posen
Solid State Sciences Laboratory

Approved for public release; distribution unlimited

Sponsored by

Defense Advanced Research Project Agency

ARPA Order 2042

Monitored by

Air Force Cambridge Research Laboratories
Air Force Systems Command
United States Air Force
Bedford, Massachusetts 01730

ABSTRACT

This report describes the results of surface damage experiments performed at 1.06 μm on proustite (Ag_3AsS_3) and at 0.694 μm on sapphire (α-Al_2O_3). A discussion of surface damage morphology of proustite for cw and pulsed illumination is illustrated using optical and scanning electron micrographs. The morphology of surface damage close to threshold suggests that the mechanism involves the absorption of laser radiation by small absorbing centers, possibly inclusions or surface impurities. Damage thresholds for proustite are presented for pulses of different durations at 1.06 μm (18 nsec and ~260 nsec) and the results are discussed in the context of a thermal mechanism. Damage thresholds of low-reflectivity sputtered alumina films on proustite were compared with thresholds for an uncoated surface of the same sample, and an appreciable increase in threshold (~40%) was observed in some cases indicating the feasibility of providing a protective film for proustite. A series of damage threshold studies on ion beam polished sapphire was performed as a continuation of work performed on an earlier program. A threshold increase of up to ten times was observed, but a large scatter in the data is evident. The total energy and temporal pulse shape of transmitted pulses at 0.694 μm have been compared with incident pulses as a function of incident power from sapphire surface damage threshold to many times higher. Results of experiments of this type are described for different focusing conditions and for different angles of incidence in air and in vacuum. A close connection with the dynamics of breakdown is evident in these data, but a detailed interpretation is not offered.

TABLE OF CONTENTS

LIST OF ILLUSTRATIONS

SECTION I

INTRODUCTION AND SUMMARY

The problem of optical damage in laser materials has been given considerable attention by a number of investigators since the early observations,[1] but in recent years the activity has been substantially increased. Because of the early use of poorly controlled multimode lasers, there was a great deal of disagreement between the reported threshold results of many workers. This was often compounded by a lack of reproducibility in material quality as well. Hence, a few years ago, it became evident that more meaningful results would be forthcoming if damage studies would be performed with carefully characterized, well-monitored lasers with smoothly varying spatial and temporal properties.

The first such investigations were initiated at Hughes Research Laboratories in an ARPA-sponsored program followed by other careful investigations at different laboratories. Bulk and surface damage in a variety of materials have been investigated under a number of different conditions and at several wavelengths. Rather than offer an extensive bibliography of published work in laser damage, we refer the reader to the proceedings of recent laser damage conferences.[2-5] The recent work performed at HRL is described in two recent contract final reports[6,7] and in a number of journal publications.[8-17]

This report contains the results of continuing experiments on laser-induced damage in optical materials. The emphasis during this period has been placed on proustite (Ag_3AsS_3) at 1.06 μm and sapphire (Al_2O_3) at 0.694 μm. In the technical discussion (Section II), we first discuss the experimental procedure used for the damage threshold measurements (Section II-A). In Section II-B, we discuss

proustite damage studies beginning with a brief survey of our earlier experimental results. This is followed by a discussion of surface damage morphology in proustite for both continuous and pulsed irradiation that is illustrated with optical and scanning electron micrographs. Optical damage in proustite for pulses of different duration is discussed next, followed by a brief description of some observations in which we discuss tentative evidence for preconditioning of proustite using low-power illumination at 1.06 μm that results in a threshold increase. Finally, experimental evidence is presented indicating that sapphire shows promise as a protective low-reflectivity coating material for proustite.

In Section II-C, we discuss a continuation of experiments already begun on an earlier program with sapphire in which it was observed that ion beam polishing results in a substantial increase (up to 10x) in damage threshold. In addition, the results of sapphire surface damage experiments are presented in which the transmitted pulses are compared with incident pulses with regard to both total energy and temporal shape. Section II-D is devoted to a description of the Nd:YAG and ruby lasers used in the program and the associated experimental setups. Section II-E presents a description of the beam diagnostics, spot size measurements, and power/energy calibration procedures used in the program.

SECTION II

TECHNICAL DISCUSSION

A. EXPERIMENTAL PROCEDURE FOR DAMAGE THRESHOLD MEASUREMENTS

In all the damage threshold measurements carried out on this program, a specific procedure was followed to obtain the desired data. The sample was prepared in a prescribed way (see below) and inspected with the aid of a microscope for cleanliness and quality of surface finish. Then it was mounted so that it could be accurately positioned relative to the focusing lens with respect to both lens-to-sample distance and to transverse position of the beam relative to any point on the surface. (A He-Ne alignment laser was used as an aid for locating the desired point on the surface in the sapphire damage experiments. It was not used with proustite because it was discovered earlier[7] that proustite is damaged by microwatt levels of illumination at 6328 Å.)

The desired location on the surface of the sample was exposed to a level of Q-switched laser illumination chosen to be appreciably below damage threshold. Then the sample was examined using a low-power (20-30x) microscope that can be moved in and out without disturbing the sample. If no damage was observed after several shots at a given level, the power was increased (by 5 to 15%) and the sample irradiated again, and so on until damage occurred. The power at which damage was seen to occur according to this procedure was taken to be damage threshold. We outline the experimental procedure in detail, because later it will be an important factor in the light of some observations made on proustite.

In all the experiments, the power and/or energy incident on the focusing lens was monitored using a photodetector-oscilloscope combination calibrated according to the procedure outlined in Section E. For the ruby laser and the low-power Nd:YAG laser, the temporal pulse shape was monitored in the damage experiments. Hence, the pulse duration could be measured for each shot. For the high-power Nd:YAG laser, however, there was insufficient signal to trigger a Tektronix 519 oscilloscope while simultaneously damaging a sample. Therefore, the pulse duration used for computing laser power quoted for the high-power Nd:YAG laser was taken as the average of a number of shots measured separately in which the full laser output was monitored with a fast silicon photodiode-519 oscilloscope combination.

The visual detection of surface damage near inception requires experience and practice in viewing through the microscope and also in choosing the proper surface illumination. It was found that many of the more subtle damages escaped visual detection in the earlier experiments because of the critical illumination requirements.

The quality of the surface finish is important, not only for determining how easily the damage can be seen, but also in determining the threshold at which damage occurs. Because proustite is so soft, it is virtually impossible to obtain an optical finish that is free of scratches by conventional abrasive polishing. In addition, a freshly polished surface that stands in air for a few hours begins to take on a cloudy appearance. This cloudiness increases slowly and is accompanied by a gradual decrease in the measured damage threshold by as much as a factor of 2 to 3 over that of the freshly polished surface.

Therefore, to obtain more meaningful and reproducible data for the detailed damage experiments, all data was taken as soon as possible after a final polish was given to a proustite sample — usually on the same day. In addition, the sample surface was lightly

repolished periodically, whenever damage thresholds were seen to begin to drift downward. After polishing and before any damage experiments were undertaken, proustite samples were rinsed thoroughly with 1,1,2 trichloroethane, followed by alcohol and finally deionized water, and then dried with a fine jet of Freon from a pressurized container. This procedure maximized the reproducibility of the experimentally obtained threshold quantities and resulted in much less experimental scatter than was obtained in earlier experiments.

B. PROUSTITE DAMAGE STUDIES

1. Survey of Early Damage Experiments in Proustite

Some attention has been given to laser-induced surface damage in proustite (Ag_3AsS_3), both at Hughes Research Laboratories and elsewhere. In an earlier program at HRL,[7] damage in proustite was studied at 1.06 μm as a function of pulse repetition rate in the range from single-shot operation to 500 pps using a repetitively Q-switched Nd:YAG laser. It was found that entrance surface damage threshold occurred at a constant pulse peak-power density (or energy density) independent of pulse repetition rate over the range studied.

The results of these experiments and single pulse data at 0.694 μm are summarized in Table I.

2. Damage Morphology in Proustite

Three distinctly different types of damage are seen on proustite entrance surfaces. The occurrence of a particular type depends on the character of the irradiation (i.e., whether pulsed or continuous) and also to some extent on the quality of the surface finish. The three types are described in the following paragraphs.

TABLE I

Damage Thresholds for Proustite as a Function of Pulse Repetition Rate

Wavelength, μm	Pulse Repetition Rate	Damage Threshold[a] Power Density, MW/cm^2		Damage Threshold Energy Density, J/cm^2	No. of Thresholds Measured
		Av Value	Range		
1.06	Single Shot	1.57	1.24 to 1.89	0.393	11
1.06	60 pps	1.61	1.40 to 1.89	0.403	11
1.06	300 pps	1.48	1.24 to 1.69	0.370	16
1.06	500 pps	1.50	1.24 to 1.73	0.376	10
0.694	Single Shot	60	54 to 69	1.08	10

[a]These values are given as total power (or energy) divided by the beam area defined as πa^2, where a is the 1/e radius for the electric field. The on-axis intensities (energy densities) are twice as large as the values quoted in the table.

T605

a. Molten Craters

These have been seen to occur only during cw illumination at relatively high cw powers or when a previously created pulse damage site is illuminated with a relatively low cw power. The formation of these craters is accompanied by a plume of yellow smoke (presumably sulfur), which sometimes settles on the undamaged surface in the vicinity of the crater, depending on the direction of air currents in the laboratory. The craters have slightly raised rims and relatively flat shiny bottoms that appear black in color and are apparently the result of molten puddles of decomposed material. Crater depth is typically 25 μm. This type of damage is the most catastrophic of the three types observed. Examples of this type of damage are seen in Figs. 1 and 2 where we present optical and scanning electron micrographs.

By being especially vigilant while irradiating the sample with continuous illumination at 1.06 μm, it is possible to cut off the light incident on the sample before the catastrophic crater formation takes place. An example of the damage formed at inception is shown in the scanning electron micrographs in Fig. 2 where we see evidence of some local melting in a region about 20 μm across.

b. Micromelting

This type of damage occurs with either single-pulsed or repetitively pulsed illumination. It is characterized by a series of somewhat randomly spaced tiny molten regions. The number and density of these regions depends on both the local surface finish and the incident power. When the power is appreciably above threshold, the molten regions merge to form a large variegated damage spot. At lower powers, there is tendency for these small globular sites to cluster along lines of surface scratches. When observed through the low-power microscope in the laboratory damage

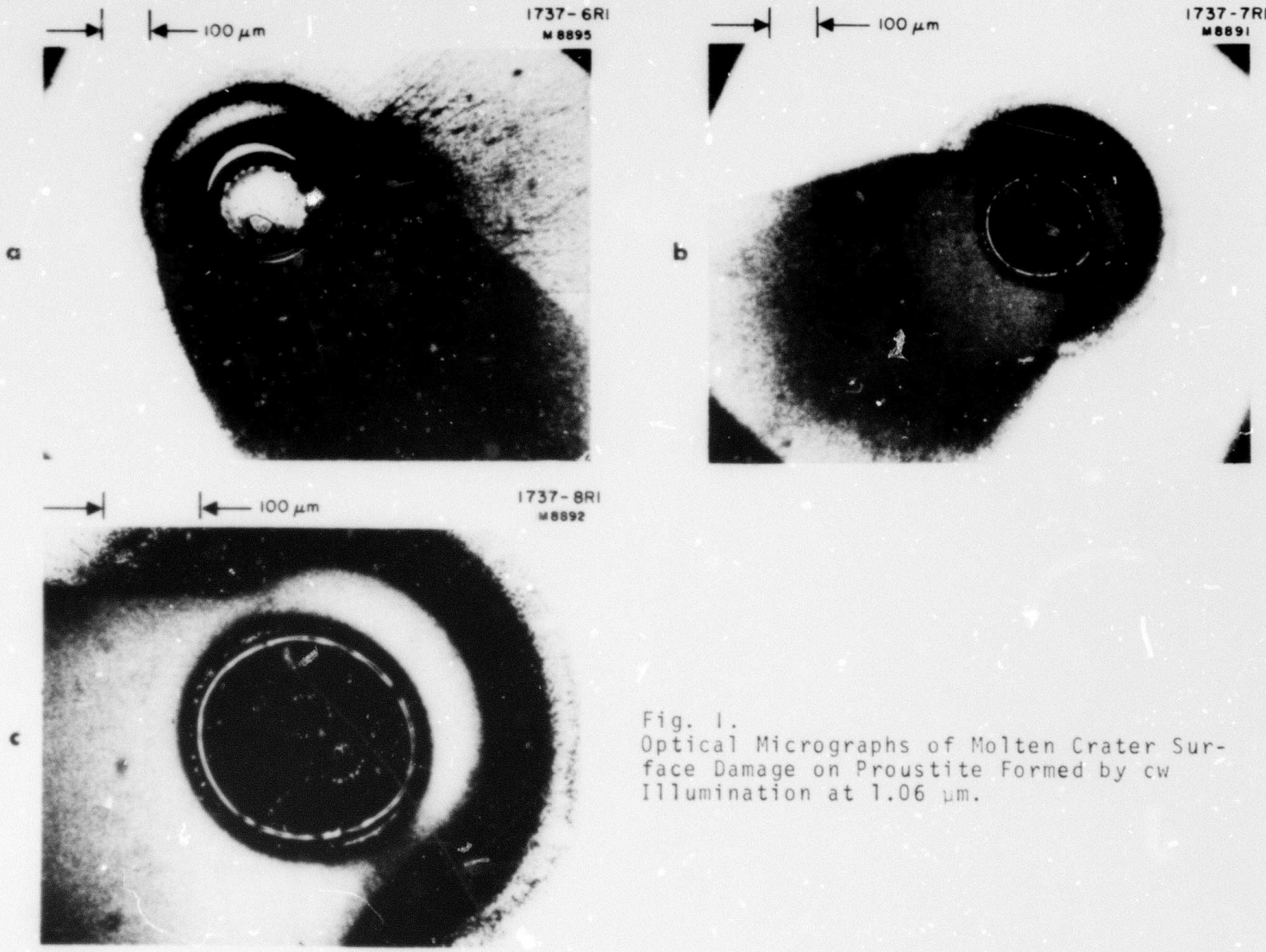

Fig. 1.
Optical Micrographs of Molten Crater Surface Damage on Proustite Formed by cw Illumination at 1.06 μm.

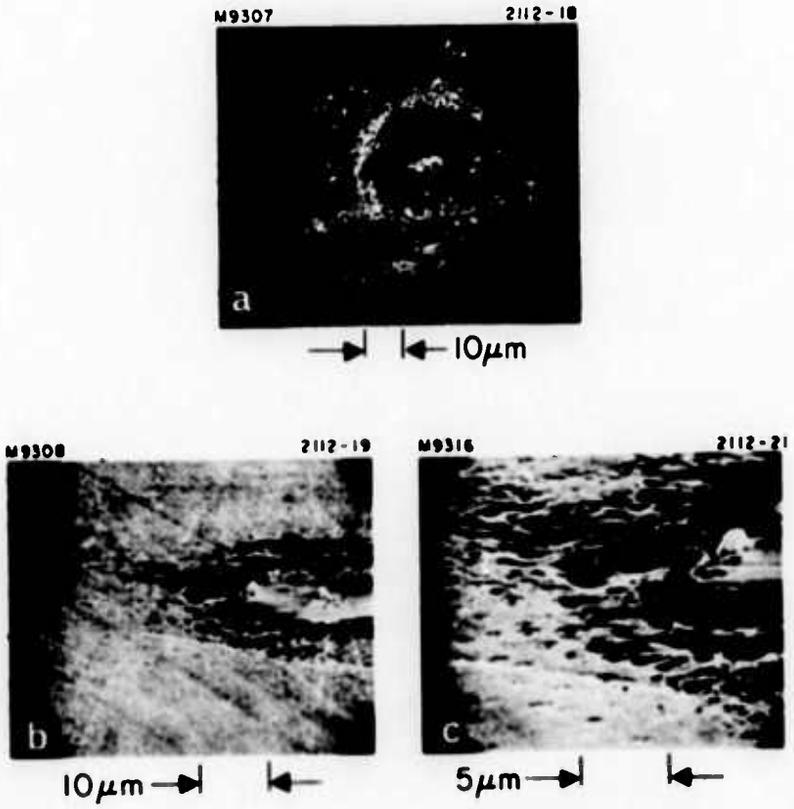

Fig. 2.
Scanning Electron Micrographs of Molten Crater Damage on Proustite Formed by cw illumination at 1.06 μm. (a) A Site Formed Close to Threshold Viewed at Normal Incidence (b) and (c) Same Site as (a) Viewed at 70° from Normal, (d) Normal View, (e) Same as (d) Viewed at 70°, (f) Normal View, (g) Same as (f) Viewed at 70°.

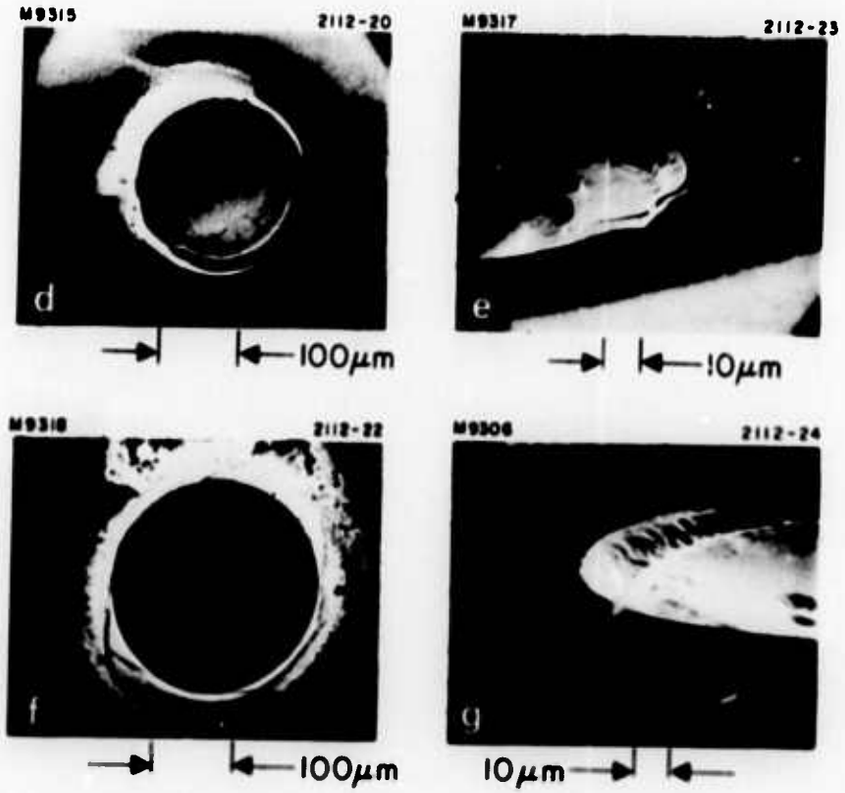

Fig. 2. Continued.

threshold setup, they appear to have a metallic luster, and the region in which they are clustered has a darker color than the surrounding undamaged surface. Figure 3 shows optical micrographs of proustite damage formed close to threshold. Figure 4 shows scanning electron micrographs of proustite damage for both single and multiple pulses.

c. Ghost Sites

This type of damage occurs with continuous illumination at 1.06 μm and was a source of much confusion when first observed. Under low magnification in the laboratory setup, it is similar in appearance to the damage described in the preceding paragraph b; that is, it appears as a speckled area with a metallic luster. This kind of damage is easily visible with the unaided eye as a small scattering region on the surface. Depending on the incident laser power and exposure time, however, the damage fades within 30 sec to 30 min after the laser is turned off and sometimes disappears completely. This type of damage happens at very low cw power, and as the power is increased, it takes longer to fade away until finally a power level is reached at which some of the damage appears to be permanent. Ghosting has been seen also at high repetition rate illumination, but only if the surface finish has the cloudy appearance referred to in the beginning of this section.

3. Optical Damage in Proustite at 1.06 μm for Pulses of Different Duration

One of the main interests for the present program has been to measure the damage threshold for proustite at 1.06 μm for pulses of different duration in an attempt to obtain some insight into the nature of the damage mechanism. This was done on the same sample using two different Nd:YAG lasers having pulse durations (FWHM)

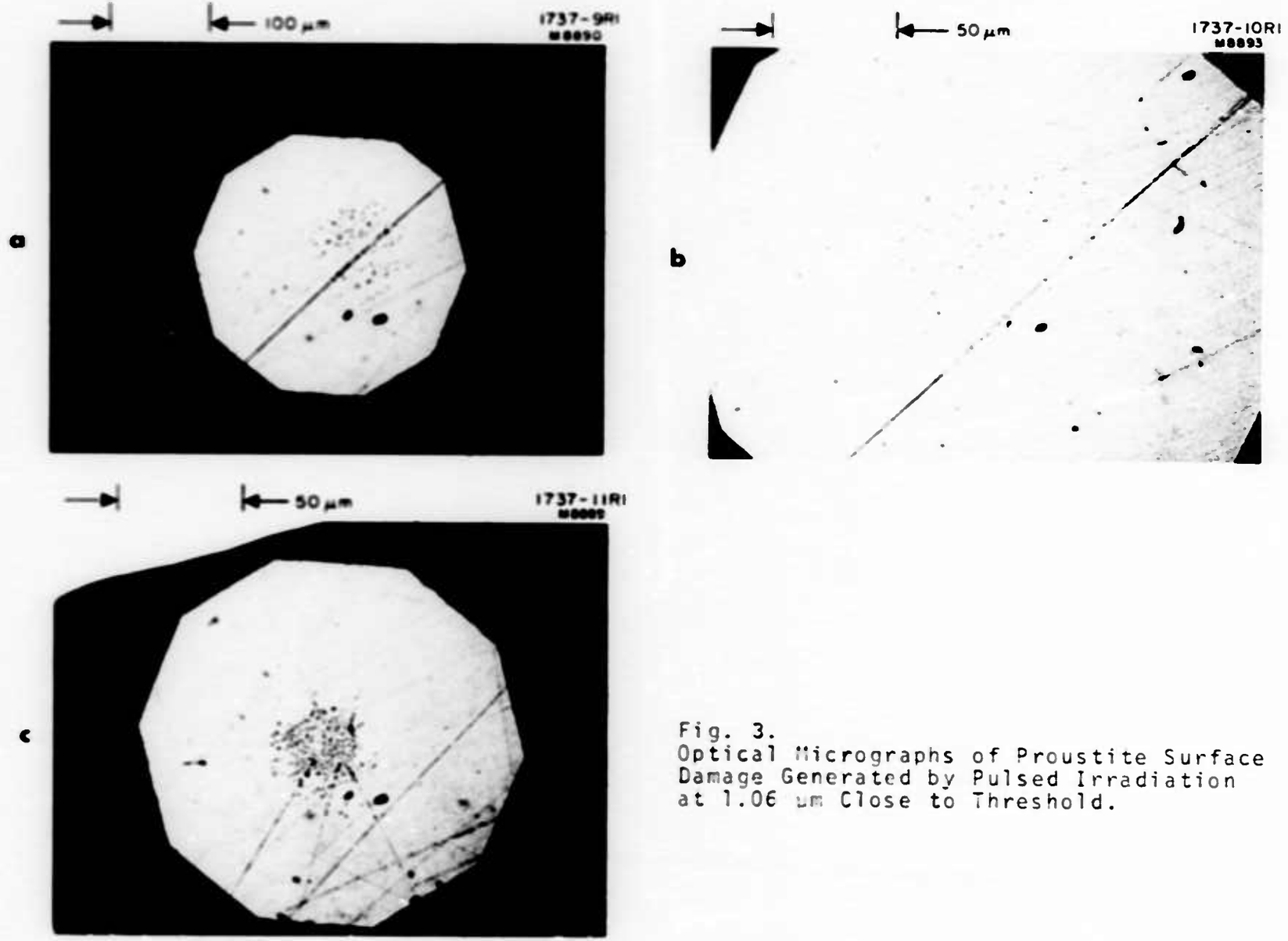

Fig. 3.
Optical Micrographs of Proustite Surface Damage Generated by Pulsed Irradiation at 1.06 μm Close to Threshold.

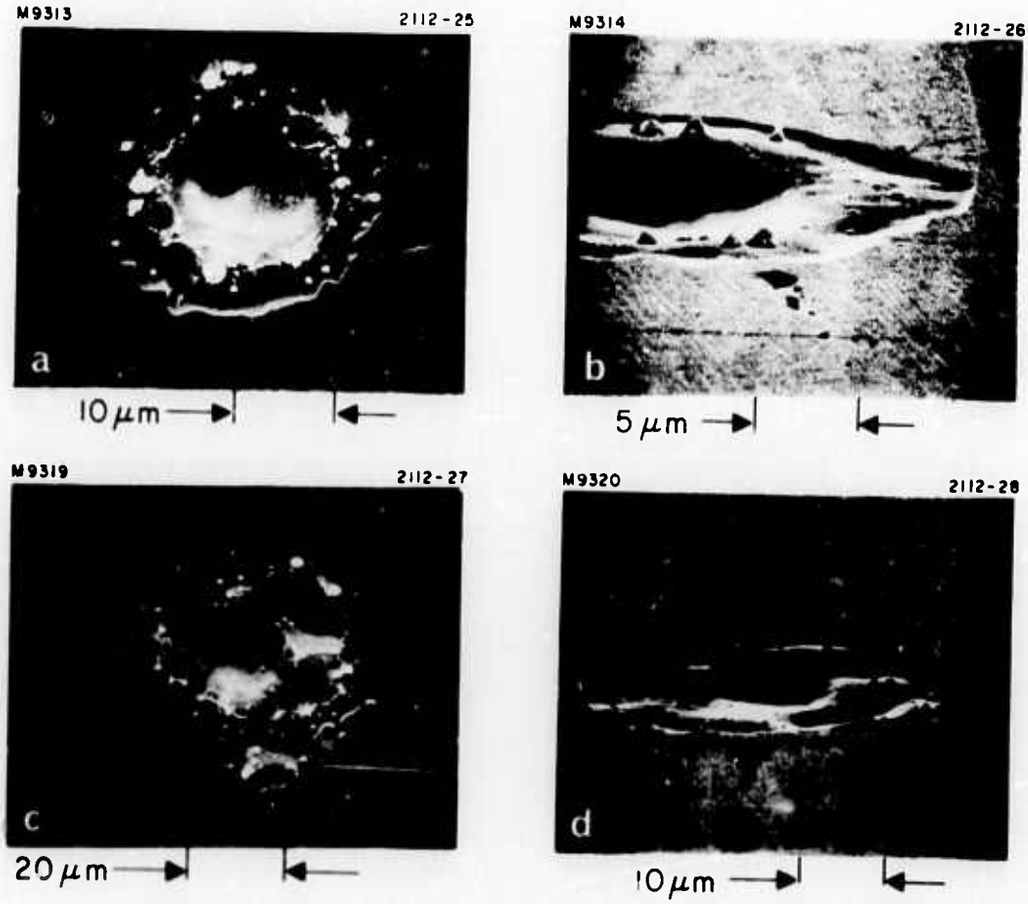

Fig. 4. Scanning Electron Micrographs of Proustite Surface Damage Generated by Pulsed Irradiation at 10.6 μm. The Picture Occur in Pairs Showing a Particular Site Viewed at Normal Incidence and at 70° from Normal. (a) Through (d) Were Formed by Single Shot, (e) and (f) were Formed by 10 Shots, (g) and (h) Were Formed by 500 pps for 1 sec.

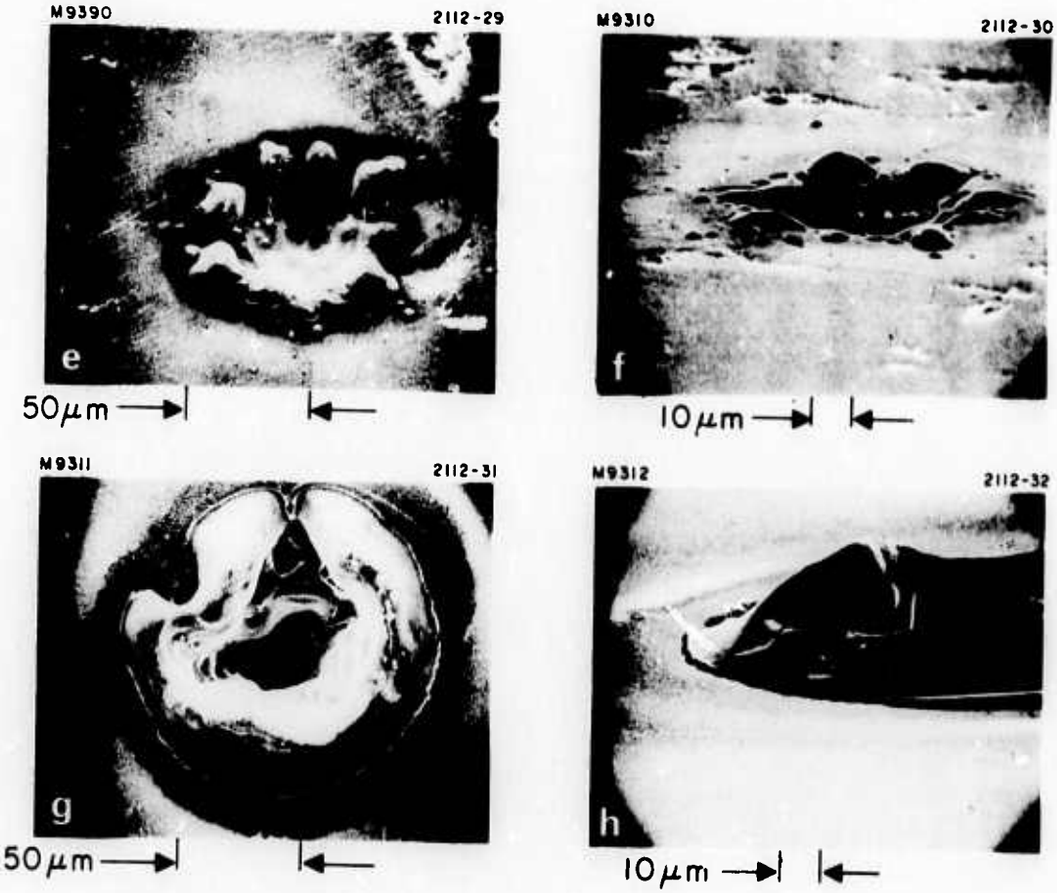

Fig. 4. Continued.

of about 20 nsec and 260 to 300 nsec. The results are presented in Table II.

We feel that while the difference in threshold values for the two pulse durations is a real one, further experimental work is required before a definitive interpretation of the data can be made. It should be pointed out also that the focused spot size at the sample surface is substantially different for the two conditions, and a possible spot size dependence cannot be ignored. However, a comparison of our results on Table II samples A and B for 17.5 nsec pulses compares favorably with those of Hanna, et al,[18] who used a laser of the same pulse duration, but substantially different focused spot size.

If we ignore for the moment the rather low value obtained in our earlier work for the 300 nsec pulse (sample C) we can qualitatively understand the differences in threshold energy density for sample A for the two pulse durations as being consistent with a thermal mechanism.

Let us consider a damage mechanism that involves the absorption of radiation and subsequent heating of the material at the surface to some critical temperature, such as the melting point at which an irreversible disturbance occurs resulting in permanent damage. Let us consider illuminating the surface with a pulse of light. If the pulse duration Δt is short compared with the time τ_c required for heat to diffuse away from the irradiated region, then there will be a critical energy density E_c for which the catastrophic temperature T_c will be reached. For all pulses of duration shorter than τ_c, one expects a <u>constant energy density</u> damage threshold. It is apparent that for pulses longer than τ_c it will be possible to deposit more energy per unit area than E_c before damage can occur, because some of the energy deposited in the first part of the pulse will have diffused away from the illuminated region before the pulse is over. Finally, in considering very long pulses (e.g., continuous

TABLE II

Entrance Surface Damage Thresholds in Proustite at 1.06 μm for Different Pulse Durations

Sample	Damage Threshold[a] Power Density, MW/cm^2		Damage Threshold[a] Energy Density, J/cm^2	Pulse Duration (FWHM), nsec	Beam Radius,[b] μm	Beam Area,[b] cm^2
	Av Value	Range[c]				
A	11.1	6.9-16.0	2.88	260-300	37.3	0.436×10^{-4}
A	40.8	31 -55	0.715	17.5	86.0	2.32×10^{-4}
B	42.1	38 -51	0.737	17.5	86.0	2.32×10^{-4}
C	1.61	1.4- 1.9	0.40	300	74.0	1.72×10^{-4}
(Ref. 18)	~40	-	0.70	17.5	650	1.33×10^{-2}

[a] These values are given as total power (or energy) divided by the beam area defined as $\pi\sigma^2$, where σ is the 1/e radius for the electric field. The on-axis intensities (energy densities) are twice as large as the values quoted in the table.

[b] Defined at the 1/e points for the electric field.

[c] These are the maximum and minimum values observed for a series of 25 to 30 measurements on a given sample.

T877

irradiation) one can achieve a nondamaging steady state in which the amount of energy per unit time being deposited is equal to the rate at which heat diffuses away from the irradiated region. This situation corresponds to a constant power density damage threshold.

The geometrical (i.e., spot size) dependence of such a damage mechanism will depend not only on the beam spatial profile, but also on whether the absorption is an intrinsic property of the material that is homogeneously distributed, or whether it is localized (e.g., inclusions or local irregularities). The morphology of proustite surface damage close to threshold suggests that the latter condition is more likely and that the absorbing regions are small compared with the beam radii employed in the experiments. Moreover, these small absorbing regions appear to occur at a sufficiently high density that there is a high likelihood of encountering many such sites in any given illuminated region.

Because past experience with different proustite samples has indicated a wide variation in properties both optical and otherwise from one sample to another, it is not surprising to see an appreciable difference in damage thresholds between different samples for the same laser pulse duration (e.g., samples A and C). In fact, it is more surprising to note the close agreement of threshold values obtained at 17.5 nsec pulse duration between our results and those of Hanna, et al.[18]

4. Pretoughening of Proustite Surfaces Using Low-Power Illumination

The study of surface damage in proustite has been further complicated by a phenomenon observed recently in this program. The following behavior was noted while performing a series of damage experiments on a freshly prepared sample (Sample A, Table II) using the low-power Nd:YAG laser. The procedure outlined

at the beginning of this section was used in obtaining data in which the desired region is irradiated with pulses of gradually increasing power until damage is observed. For several spots on the surface that were irradiated with a large number of low-power shots (15 to 20), we were unable to obtain damage with repeated pulses at the maximum power available from the laser. When the sample was moved slightly, so that the beam was allowed to strike a spot only about 50 μm away from the previously nondamagable location, damage invariably occurred on the first shot. Subsequent to observing this behavior, we carried out a different series of experiments where we held the output of the laser constant for a series of shots, each time hitting a different spot on the surface and examining for damage between shots. This was done over a range of incident power levels with about 20 shots taken at each level. In this series, damage was found to occur, on the average, at lower levels (30% lower) than for cases where the sample was preirradiated at low nondamaging powers.

This behavior was further complicated by the general gradual surface degradation always observed with proustite with exposure to the laboratory environment. Hence, after a few hours the preconditioning phenomenon seemed to disappear, or at least diminish appreciably to the point that the occurrence of damage at a given level seemed to be independent of whether or not the spot of interest had been preirradiated at lower levels.

We point out this behavior as an additional illustration of the complexity of damage behavior in proustite.

5. Surface Damage on Al_2O_3-Coated Proustite

Recently in another program[7] the idea arose that it might be advantageous to provide a protective coating for proustite

that would result in better damage properties.* The combined facts that sapphire (Al_2O_3) has a high damage threshold and a refractive index (1.76) that is close to the geometric mean between that of proustite (~3) and air made it a good potential candidate as a low-reflectivity, damage resistant coating for proustite.

Early preliminary experiments using the low-power Nd:YAG laser indicated that the sapphire-coated surface had a higher damage threshold than the uncoated surface. The results were inconclusive, however, because there was a lot of scatter in the data; some spots on the surface would not damage with the maximum output from the laser while others were damaged at the same level as the uncoated surface. Also, the quality of the coatings was not as good as it was felt could be achieved. Hence, it was decided to perform more detailed damage experiments on the better quality coatings that became available during this program. A wafer of proustite about 15-mm diameter and 2-mm thick was coated in three different regions with Al_2O_3 coatings of different thicknesses: 1450 Å, 1700 Å, and 1970 Å which correspond to 0.24λ, 0.28λ, and 0.33λ at 1.06 μm. A fourth region of the sample remained uncoated.

Damage threshold measurements were made on all four regions of the sample using the high-power Nd:YAG laser (pulse duration 17.5 nsec) focused on the entrance surface. The results of these measurements are presented in Table III.

The damage threshold energy and power densities listed in the second and third columns of Table III are the measured values incident upon the sample surface. However, because a fraction of the light is reflected from the sample, the actual energy available

---

*This concept arose in a discussion with H. L. Garvin of HRL who has provided the sputtered Al_2O_3 coatings that have been studied on this program

TABLE III

Damage Thresholds for Al_2O_3-Coated Proustite

Region	Al_2O_3 Coating Thickness, Å	Damage Threshold[a] Energy Density, J/cm^2	Damage Threshold[a] Power Density, MW/cm^2	Measured Transmission, T	Intensity Reflection Coefficient at Entrance Surface, R	Corrected Threshold[a] Energy Density, J/cm^2
A	Uncoated	0.737 ± 6.5%[b]	42.1	0.324 ± 0.010[b]	0.204	0.587
B	1450	0.858 ± 8.9%	49.0	0.398 ± 0.018	0.0238	0.838
C	1700	0.729 ± 8.3%	41.5	0.413 ± 0.023	(-0.0151)	0.729
D	1970	0.615 ± 10.6%	40.2	0.402 ± 0.013	0.0134	0.607

[a] These values are given as total power (or energy) divided by the beam area defined as $\pi\alpha_0^2$, where α is the 1/e radius for the electric field. The on-axis intensitites (energy densities) are twice as large as the values quoted in the table.

[b] The values listed are the average deviations taken from 25 to 30 measurements for each region.

T878

at the surface for creating damage should be multiplied by the quantity 1-R, where R is the intensity reflection coefficient. Therefore, a more valid comparison of the entrance surface damage thresholds for the coated regions compared with the uncoated region will account for the difference in entrance surface reflectivities.

The reflectivities of the coated surfaces were not measured directly, but they can be obtained by a comparison of the measured transmissions as listed in the table. The energy transmission T of a slab of absorbing material having reflection coefficients at the entrance and exit surfaces of R_1 and R_2, respectively, is given by

$$T = \frac{(1-R_1)(1-R_2)e^{-\alpha d}}{1-R_1R_2e^{-2\alpha d}} \tag{1}$$

where d is the sample thickness and α is the absorption coefficient.

For region A (uncoated), $R_1 = R_2$ and we can compute the absorption $e^{-\alpha d}$ from the measured transmission value, T_1

$$T_1 = \frac{(1-R_1)^2 e^{-\alpha d}}{1-R_1^2 e^{-2\alpha d}} \tag{2}$$

Rearranging (2) and solving for $e^{-\alpha d}$ we obtain

$$T_1R_1^2e^{-2\alpha d} + (1-R_1)^2e^{-\alpha d} - T_1 = 0 \tag{3}$$

$$e^{-\alpha d} = \frac{(1-R_1)^2}{2R_1^2T_1}\left[-1 + \left(1 + \frac{4T_1^2R_1^2}{(1-R_1)^4}\right)^{1/2}\right] \tag{4}$$

Because the second term under the square-root radical is small compared to unity (~0.04), the radical can be expanded using $(1 + x)^{1/2} \cong 1 + 1/2x$ for small x and (4) simplifies to

$$e^{-\alpha d} \cong \frac{T_1}{(1-R_1)^2} \tag{5}$$

We assume that the absorption is uniform throughout the sample and use the expression

$$R_1 = \left(\frac{n-1}{n+1}\right)^2 \tag{6}$$

to obtain the reflectivity of the uncoated surface. Here we use the value n = 2.65* for proustite, obtaining the value $R_1 = 0.204$.

To obtain the reflectivity for a particular coated region of the sample, we solve (1) for R_2 and obtain

$$R_2 = \frac{(1-R_1)e^{-\alpha d} - T_2}{(1-R_1)e^{-\alpha d} - T_2 R_1 e^{-2\alpha d}} \tag{7}$$

Here, T_2 is taken to be the measured transmission through the coated region of the sample. Substituting in (7) for $e^{-\alpha d}$ from (5) we obtain

$$R_2 = \frac{1 - T_2(1-R_1)/T_1}{1 - T_1 T_2 R_1/(1-R_1)^3} \tag{8}$$

---

*Proustite is birefringent with ordinary and extraordinary indices $n_o = 2.75$ and $n_e = 2.55$. We have taken n = 2.65 because the orientation of the sample was not determined. The values of R_1 computed using n_o and n_e respectively, are 0.207 and 0.191; the difference between these values is well within the experimental error of the transmission measurements.

The reflectivities listed in Table III for regions B, C, and D are computed from (8). The small negative reflectivity listed for region C is not real, of course, but a result of the experimental error in measurement of the transmissions and the assumption that the absorption and reflectivity are uniform throughout the sample.

The corrected threshold energy densities listed in Table III are obtained by multiplying the appropriate measured values by $(1-R_1)$. Here we see that all three coated regions have thresholds higher than the uncoated region, although the values for regions A and D lie within experimental error of each other.

In all cases, the damage of Al_2O_3-coated proustite occurs at the interface between the coating and the surface. Examples of this damage are given in Fig. 5. Figure 5(a) through (d) show examples of damage formed when the sample was irradiated at a level fairly close to threshold, while Figs. 5(e) and (f) are examples of damage found 2 to 3 times threshold. Figure 5(a) shows damage in the vicinity of a scratch on the proustite surface where the alumina film became separated from the surface prior to the damage formation. In all cases illustrated, the damage appears as small molten globules similar to that seen on the uncoated surface accompanied in most instances by film separation.

The moderate increase in threshold observed in some instances for sapphire-coated proustite offers some promise as a protective coating, but it is evident that the quality of the proustite itself must be improved with regard to both freedom from impurities and inclusions and quality of surface finish. The nature of the observed damage morphology suggests very strongly that the damage threshold values obtained so far are not a measure of the <u>intrinsic</u> damage resistance of proustite, but indicate a limitation governed by impurities and/or inclusions as well as surface fabrication.

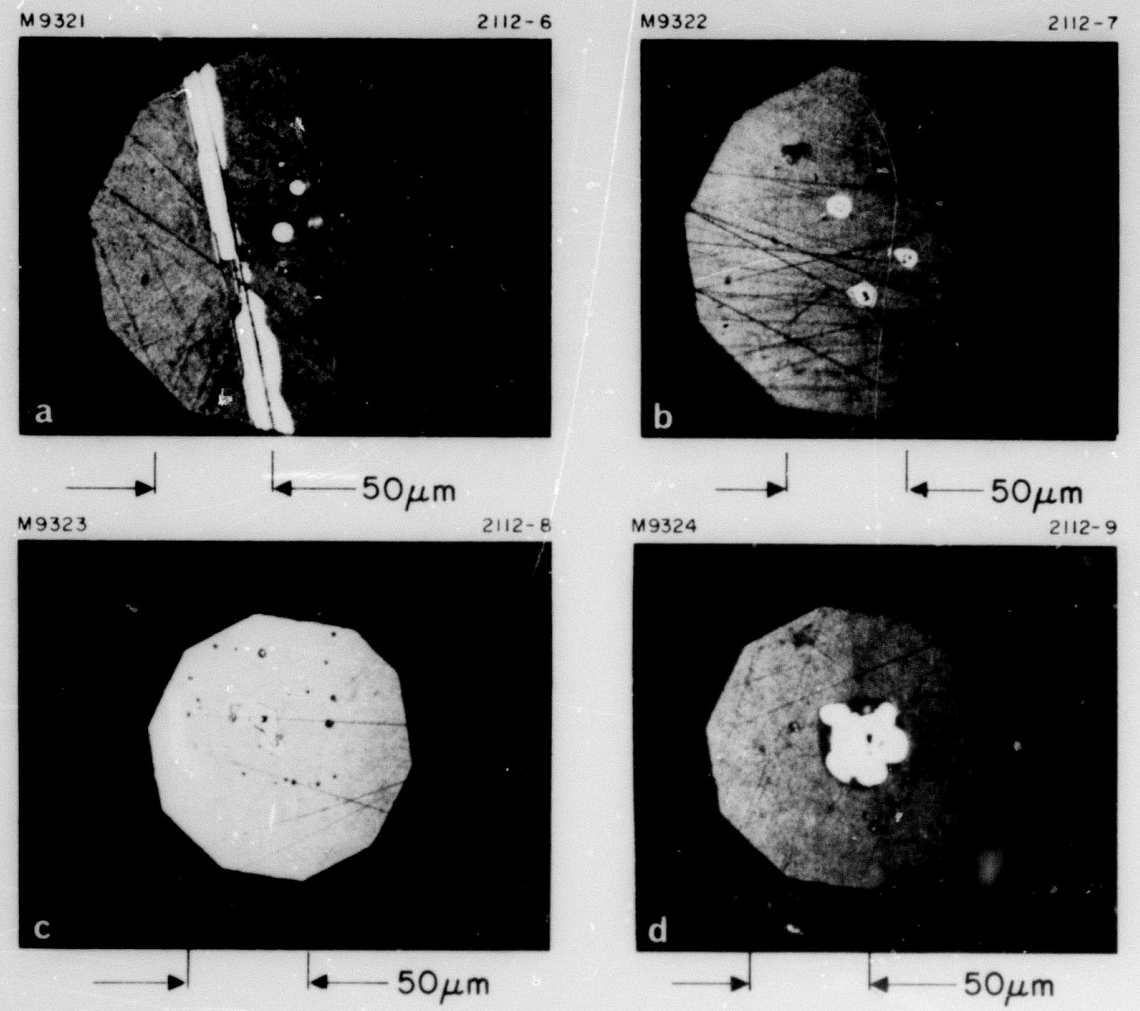

Fig. 5. Optical Micrographs of Damage on Sapphire-Coated Proustite Surface.

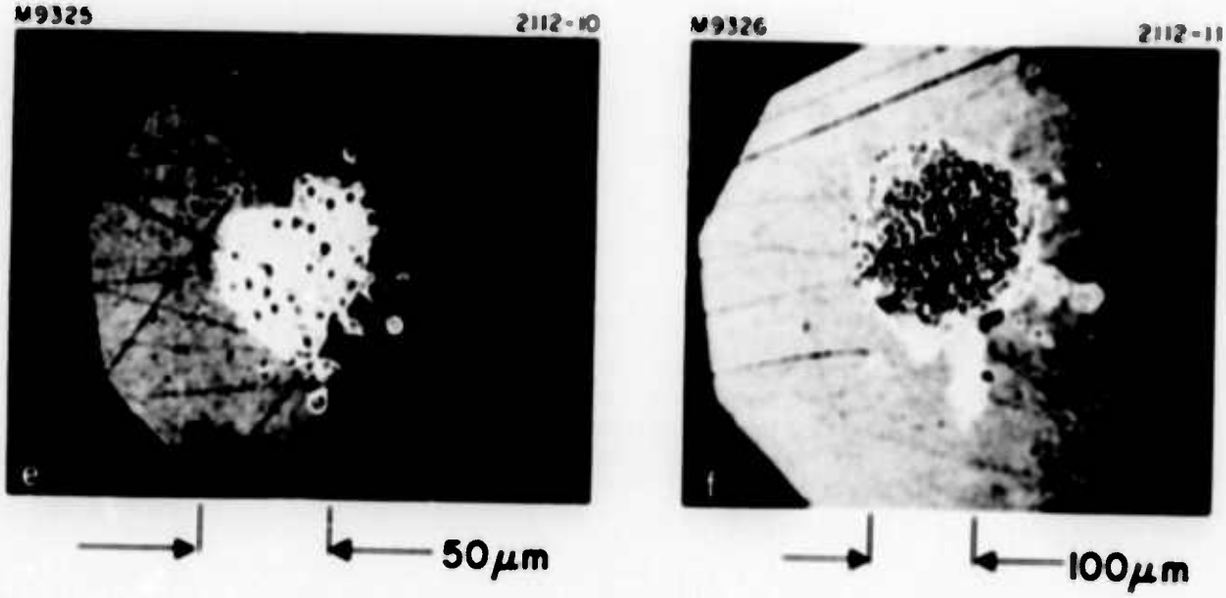

Fig. 5. Continued.

C. SAPPHIRE STUDIES

1. Surface Damage Threshold Measurements in Ion Beam Polished Sapphire

On an earlier program,[6, 12] work was initiated on the use of ion beam polishing as a means of improving the surface damage resistance of optical materials. The main emphasis for these treatments was placed on sapphire. A number of experiments were performed for different conditions of ion polishing, and a distinct improvement was obtained, but the need for further work was evident and some additional experiments have been carried out on this program. These are described below, following a brief discussion of the earlier work.

All the experiments were carried out using the single-mode, Q-switched ruby laser described in Section D-3, and the experimental setup described schematically in Fig. 14. The light is focused with a 19-cm focal length lens onto the surface-of-interest of the sapphire sample whose typical dimensions are 3 in. long by 0.25 in. square cross section.

A typical series of measurements is carried out as follows: The laser is fired at a particular spot on the desired surface at a power below damage threshold. Then the sample is examined through a traveling microscope without disturbing the sample between shots. If no damage is observed, the incident power is increased (by ~10%-20%), and again the sample is examined. The procedure continues until damage is observed; then the sample is moved and the process repeated on an undamaged spot. Typically 10 to 20 damage thresholds are measured in this way for a given surface.

Abrasively polished samples were used as obtained from the manufacturer (Union Carbide). They were fabricated with the laser finish specifications typical for ruby laser rods. Ion polished samples were exposed after mechanical processing to an Ar^+ beam

(7 kV, 300 $\mu A/cm^2$) for periods from 2 to 4 hr. The beam strikes the surface at an angle of 20° from the surface plane. An estimated 200 Å/min is removed from the sapphire surface under these conditions giving a total of about 2.5 to 5 μm of material removed in a given exposure.

Results of the early measurements on abrasively polished samples compared with ion polished samples are shown in Fig. 6. Figure 6(a) shows the exit damage thresholds for the abrasively polished sample. Here, most of the observed damage occurs between 1 GW/cm^2 and 2 GW/cm^2. For the ion polished case (Fig. 6(b)) the exit damage threshold values are distributed over a wide range, but no damage thresholds lower than 2 GW/cm^2 are observed. (The data shown in Fig. 6(b) were obtained from samples that were ion polished for 2 and 4 hr. Because no noticeable change in the distribution was observed for the two conditions, the data are presented together in the figure.) The results for entrance surface damage are shown in Fig. 6(c) and (d). For the abrasively polished sample, most of the damage thresholds occur between 1 GW/cm^2 and 2.5 GW/cm^2 with a few higher values observed. For the ion polished case (Fig. 6(d)), we see a few damage thresholds ranging from 2 GW/cm^2 to 9 GW/cm^2 with a large fraction (> 50%) occurring above 10 GW/cm^2. The dashed portion of Fig. 6(d) indicates that we were unable to reach damage threshold with the maximum output from our laser under the focusing conditions of our experiment.

One of the main reasons for continuing the study of damage in ion polished sapphire was to obtain additional high-power points for Fig. 6(d). For this we used the ruby amplifier described in Section D-3 that was not employed in the earlier measurements. The results of these experiments are shown in Fig. 7(d) with the earlier data for comparison. Here we see damage thresholds that range up to >20 GW/cm^2. The sample used in these experiments was ion polished for 8 hr under the same conditions of ion energy and current

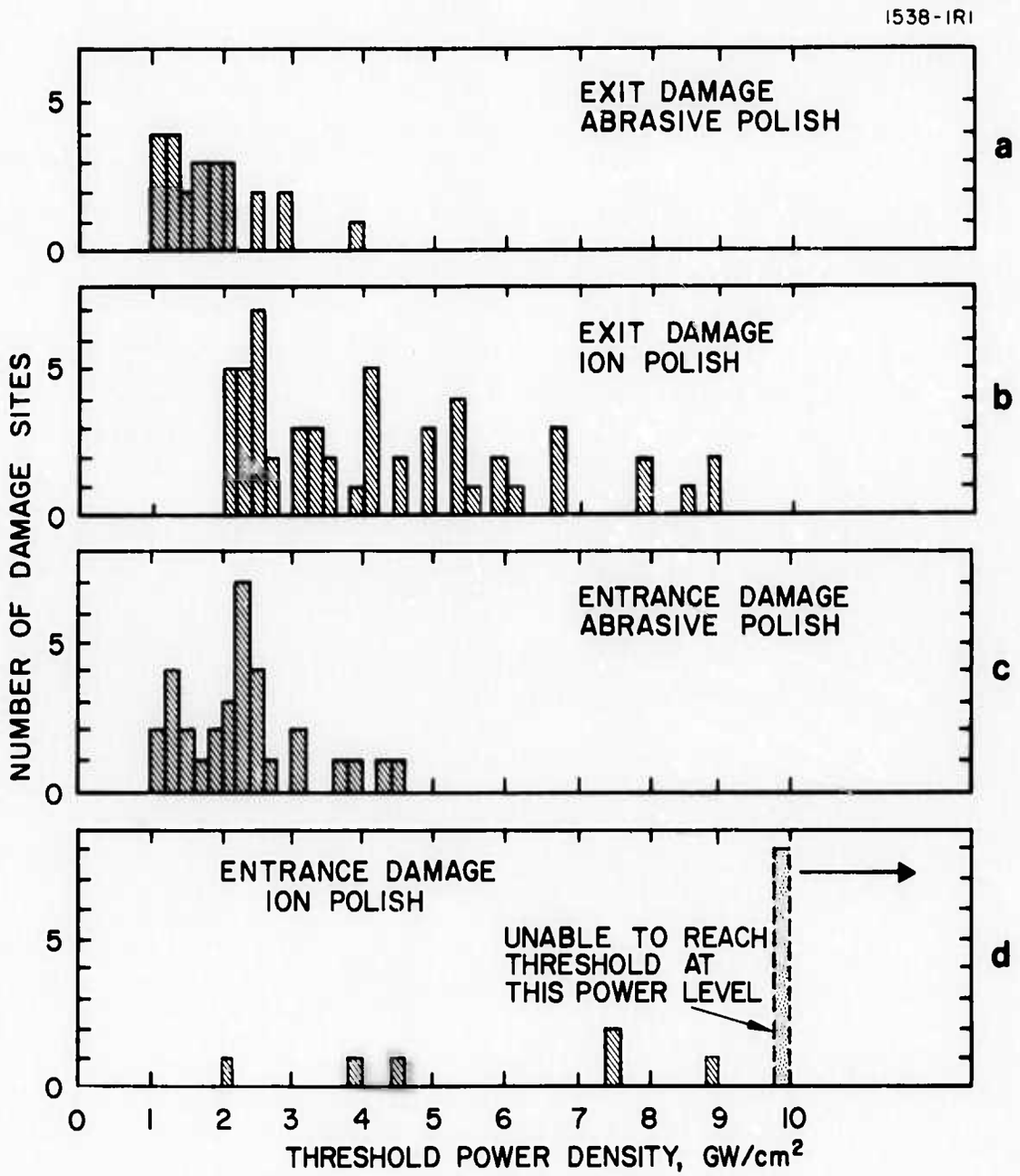

Fig. 6. Histograms of Early Data Comparing Damage Thresholds for Ion Polished Sapphire to Abrasively Polished Sapphire.

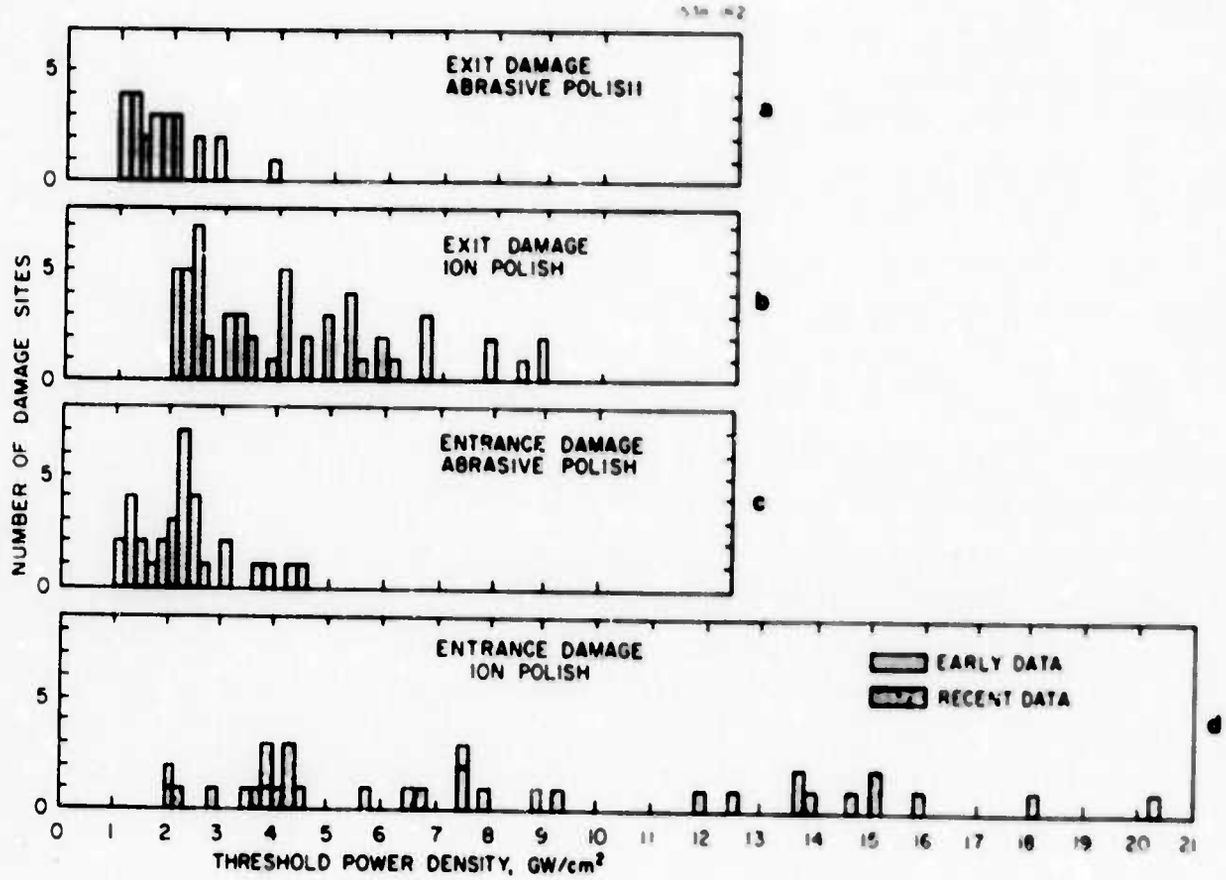

Fig. 7. Histograms of Fig. 6 Including New Data for Entrance Damage on Ion Polished Sapphire.

as used earlier. The reason for the longer ion beam exposure was to see whether the scatter observed in the earlier threshold data might be reduced somewhat for a longer treatment. We see that this is not the case.

The reason for the large scatter in the threshold data for the ion polished samples compared with that for the abrasively polished samples is not known, although a likely interpretation is that while a distinct improvement in surface quality is gained by ion beam polishing, the improvement is not uniformly distributed over the surface. This improvement in surface quality could be related to either the removal of surface irregularities such as the fine scratches that arise from abrasive polishing, or to the improvement in surface crystallinity as evidenced by X-ray topographs, or both these factors.

Bloembergen[19] has pointed out that the optical electric field strength in the neighborhood of surface features, such as cracks and micropores, can substantially lower the threshold for electric avalanche breakdown on the surface of transparent dielectrics. A possible interpretation of the scatter in thresholds for the ion polished samples compared with the abrasively polished sample is that, in the latter case, the surface quality is uniformly poor, resulting in a relatively narrow spread of damage thresholds. For the ion polished surfaces, however, a distinct improvement in quality is attained with regard to both improved crystallinity and removal of scratches, but this improvement is not uniform over the surface and a broader range of thresholds is observed.

2. Comparison of Transmitted-to-Incident Light During Damage Generation

From time to time the questions have arisen – What fraction of the incident light pulse is consumed in the damage process? and, What is the temporal shape of the transmitted damaging pulse?

We have attempted to answer these questions with respect to surface damage in sapphire and proustite. To accomplish this, we have placed a diffuse reflector (MgO) beyond the sample being damaged and monitored the transmitted light in both time-resolved and time-integrated fashion. Hence, we have obtained data that give us the total integrated energy transmission of the sample during the damaging process as well as the temporal shape of the transmitted pulse.

Experiments on sapphire were done for both entrance and exit surface damage using three different lenses whose focal lengths were 3.8 cm, 7.6 cm, and 19 cm. Qualitatively, all the phenomena observed were the same for the different focusing conditions.

Figure 8 shows the percent-transmission as a function of power density incident on the entrance surface of sapphire. The light is focused on the entrance surface using the 19-cm lens. Integrated signals from each of two detectors proportional to the incident and transmitted light, respectively, are displayed on each trace of a Tektronix 555 dual beam oscilloscope. The ratios of the signals are measured for each shot with the sample in place and compared with the ratio when the sample is not present. We see from Fig. 8 that the percent-transmission at damage threshold (1.6 GW/cm^2) drops sharply from 84 to 86% to the range 55 to 65%. As the incident energy is increased, we observe a monotonic decrease in transmission that appears to level off around 5% transmission. Similar data for shorter focal length lenses taken in less detail show the same qualitative behavior.

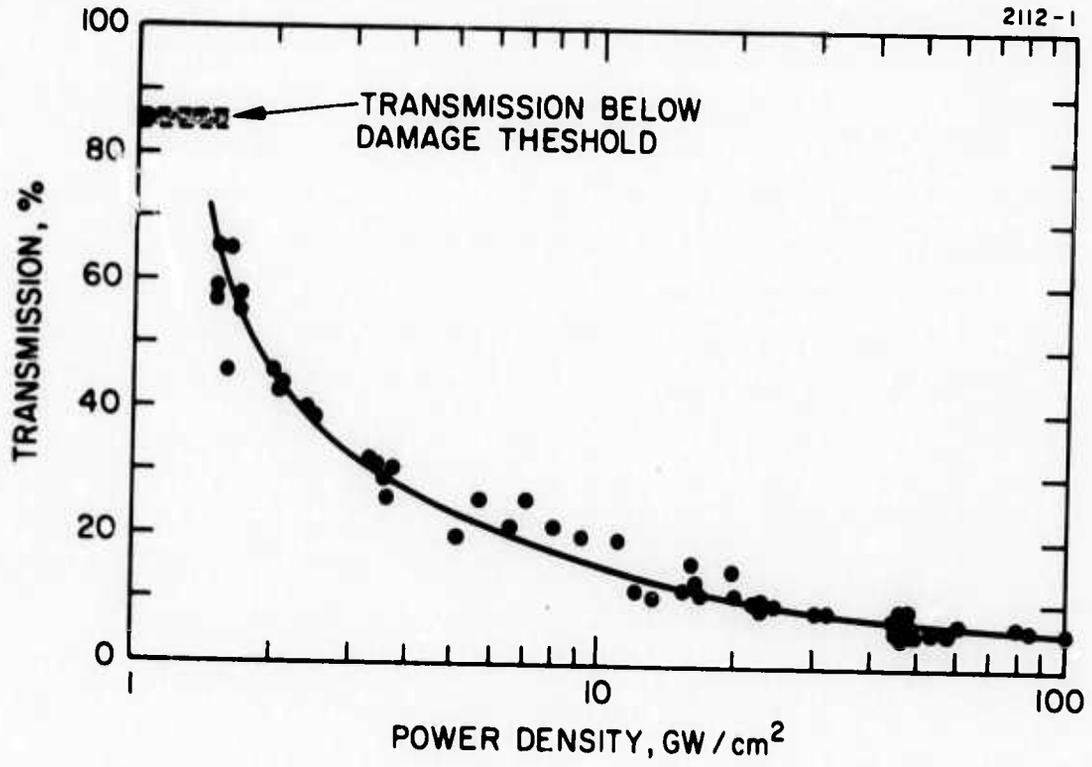

Fig. 8. Percent of Total Energy Transmission at 6943 Å Versus Incident Power Density of Light Focused at the Entrance Surface of a Sapphire Sample.

When the temporal behavior of the transmitted pulse is examined close to threshold, a similar behavior to that for air breakdown plasmas is observed, namely a sharp cutoff of the incident pulse at the time breakdown occurs. However, even close to breakdown threshold, an appreciable amount of the remainder of the pulse continues to be transmitted through the damage surface plasma.

In Fig. 9, we present a series of oscilloscope traces showing the temporal shape of the transmitted laser pulse for increasing incident power. For comparison on each photograph we show also a second trace taken at the same power on a separate shot with the sample removed from the beam. Thus each photograph gives an indication of the time at which the surface plasma forms as well as an indication of the degree to which different parts of the pulse are attenuated.

One qualitative feature of interest in the photographs in Fig. 9 is that at higher powers the initial cutoff is less steep than at lower powers and an increasing fraction of the remainder of the pulse is transmitted relative to the part that was transmitted before breakdown occurred. The reason for this increase in transmission later in the pulse is likely to be related to the dynamics of formation and expansion of the surface plasmas, but more information is needed to provide some understanding of the details of this phenomenon.

All the qualitative temporal features shown in Fig. 9 are observed for both entrance and exit damage in sapphire. They are also seen when the sample is placed in a vacuum chamber with the entrance surface tilted with respect to the incident beam. Recent studies at HRL[6, 14, 16] have shown that there is more than one type of laser-induced surface plasma. The plasma that occurs at the entrance surface has two components that can be distinguished both spatially and temporally. One component is an air plasma that is always found in the direction of the incident light beam. This component is not present when the entrance surface is damaged in

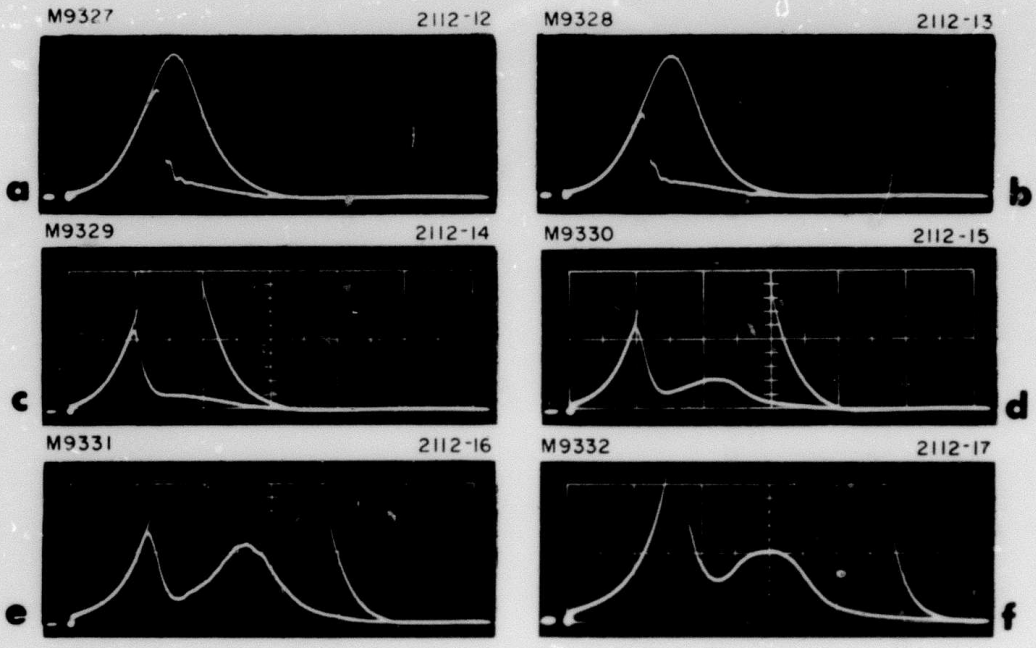

Fig. 9. Oscilloscope Traces Showing Transmitted Pulse Shape Through Sapphire During Damage Formation Compared with Pulse of Same Energy with Sample Removed. Sweep Rate - 10 nsec/div. Incident Power Times Threshold (a) ∿1.2x, (b) ∿2.5x, (c) ∿4x, (d) ∿12x, (e) ∿20x, (f) ∿100x.

a vacuum. The second component is always spatially directed normal to the sample surface, no matter at what angle the light strikes the surface. The fact that we observe the same transmitted-pulse temporal shape for the sample tilted in vacuum as in air indicates that the dynamics of the air-sustained plasma are not responsible for the temporal characteristics. Further work on this interesting phenomenon will certainly provide a deeper understanding of the details of the damage phenomenon.

D. LASERS USED IN DAMAGE STUDIES

1. High-Power Nd:YAG Laser

The high-power Nd:YAG laser (as schematically illustrated in Fig. 10) is pulse-excited by a Kr-arc pump lamp and electro-optically Q-switched. It has the capability of being triggered externally from single-shot operation to maximum repetition rate of 10 pps or internally triggered at 10 pps. The Nd:YAG rod is 0.25-in. diameter by 2-in. long, pumped by the 2-in. arc length Kr lamp in a close coupling configuration. The output coupler is a flat 47% transmission mirror, and the high reflector (HR) used is a 53-cm radius-of-curvature mirror. To achieve single transverse mode control, the resonator cavity is internally apertured by a 2-mm diameter pinhole placed 14 cm from the HR mirror. The laser resonator is 52 cm in length.

At full output (i.e., no transverse mode control), the output energy is approximately 100 mJ/pulse with about a 20-nsec pulse-width. However, when apertured to produce the desirable transverse mode profile, the output energy is reduced to about 7 mJ/pulse with an 18.5-nsec pulsewidth. For single-shot operation, there exists a ±3% amplitude fluctuation in the pulse height from shot to shot. When operated at 10 pps, the amplitude fluctuation disappears

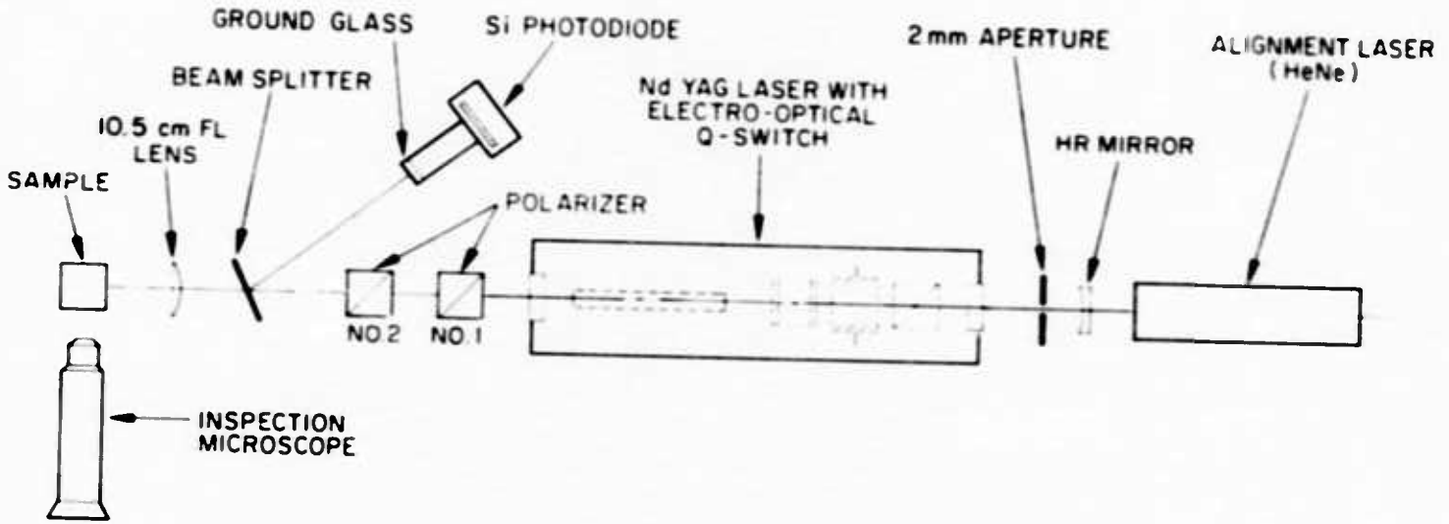

Fig. 10. Experimental Setup for Damage Experiments Using High-Power Nd:YAG Laser.

and the output is very stable. Since no longitudinal mode control is employed, the pulse is temporally modulated with amplitude and frequency varying somewhat from shot to shot. Oscilloscope traces illustrating this modulation for a series of 8 consecutive shots are shown in Fig. 11.

2. Low-Power Nd:YAG Laser

The low power Nd:YAG laser as schematically shown in Fig. 12 is continuously pumped by a Kr-arc lamp and acousto-optically Q-switched. It has the capability of being operated continuously, single pulsed, or repetitively Q-switched at rates up to 50 kHz. The pump cavity utilizes an elliptical 2-in. long cylinder with walls coated with evaporated gold. The Nd:YAG rod is 0.25-in. diameter by 2-in. long, while the Kr-arc lamp discharge is 2-in. long with a 4-mm bore diameter.

The resonator cavity is formed by two 1-m radius-of-curvature mirrors separated by a distance of 65 cm. For the experiments, a 4.2% transmission output mirror was used. An internal aperture of variable diameter provided the transverse mode control. By decreasing the aperture size, the TEM_{00} output mode of the laser can be obtained by progressively eliminating the higher order transverse modes. The TEM_{00} is then selected with the collapse of the degenerate TEM_{10} mode. A UV-excited IR phosphor screen is utilized for visual selection of the TEM_{00} mode.

At full power, multimode output of 54 W is obtainable using a single 2.5-kW Kr-arc lamp. However, due to the well-known thermally induced birefringence of the Nd:YAG rod, the TEM_{00} output was drastically reduced to approximately 1.5 W maximum. (No attempt was made to compensate the induced birefringence.) This resulted in peak powers of about 1 kW at low repetition rates (<500 pps). The peak power decreased monotically for high repetition

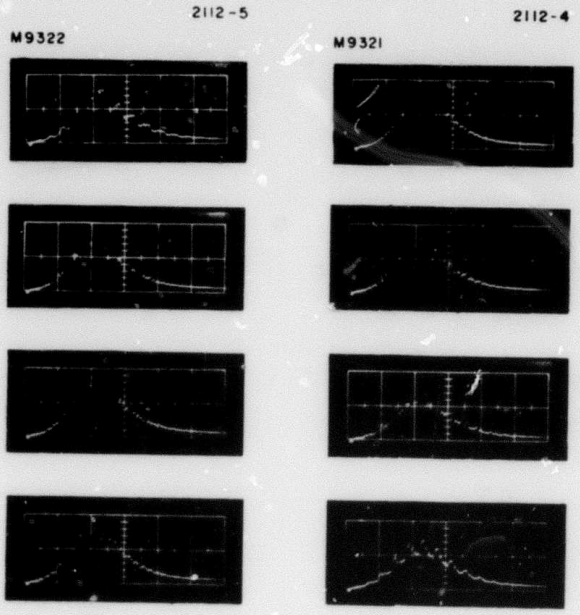

Fig. 11.
Typical Oscilloscope Traces of Output from Eight Consecutive Shots of High-Power Nd:YAG Laser. Sweep Rate - 10 nsec/div.

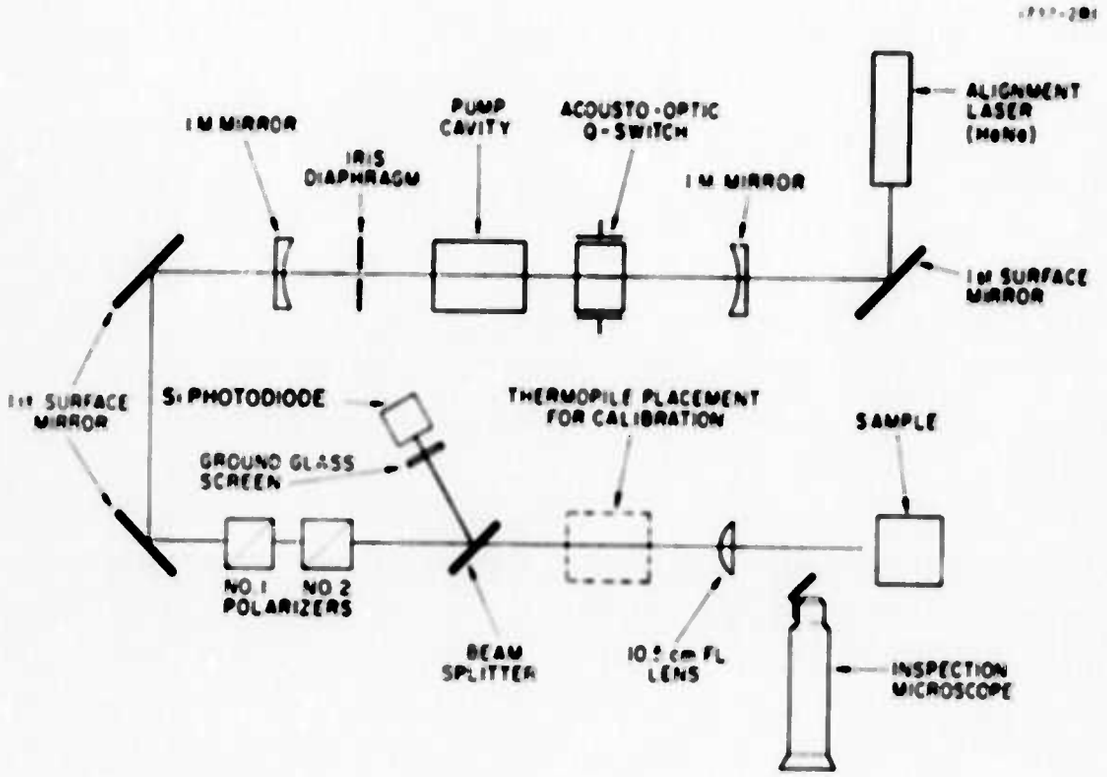

Fig. 12. Experimental Setup for Damage Experiments Using the Low-Power Nd:YAG Laser.

rates. Pulsewidths of between 180 to 300 nsec resulted, depending on the repetition rate used. Amplitude stability was ~ ±3% when the laser was properly adjusted. An oscilloscope photograph of a number of single shots showing the typical reproducibility for this laser is shown in Fig. 13.

3. High-Power Q-Switched Ruby Laser

The experimental setup is shown in Fig. 14. The oscillator employs a 4-in. long by 0.25-in. diameter ruby, pumped by two linear lamps in a double elliptical pump cavity. The ruby crystal is water cooled by a closed cycle refrigeration system maintained at 0°C. The high reflectivity mirror is coated with a 99+% reflectivity high-field damage coating from Perkin Elmer Corporation. Q-switching is accomplished with a solution of cryptocyanine in methanol in a 1-mm path-length cell whose transmission is 30% at 6943 Å. The 2-mm aperture allows oscillation in the TEM_{00} mode.

The temperature controlled (34°C) resonant reflector that was designed to optimize longitudinal mode control consists of two quartz etalons and a quartz spacer, whose combined effect is to enhance cavity modes separated by 2 cm^{-1} and to discriminate against intermediate modes.

Portions of the laser beam are split off in various ways (see Fig. 14), so that the power output, near and far field patterns, and Fabry-Perot patterns can be monitored for each shot. An oscilloscope trace of a typical output pulse for this laser is shown in Fig. 15.

The water-cooled amplifier ruby is 6-in. long by 0.5-in. diameter, with one end wedged relative to the other by about 0.5°. The input end of the amplifier rod is antireflection coated to minimize the chances of oscillation within the amplifier itself. The ruby rod is closely coupled to a helical flashlamp, which is pumped

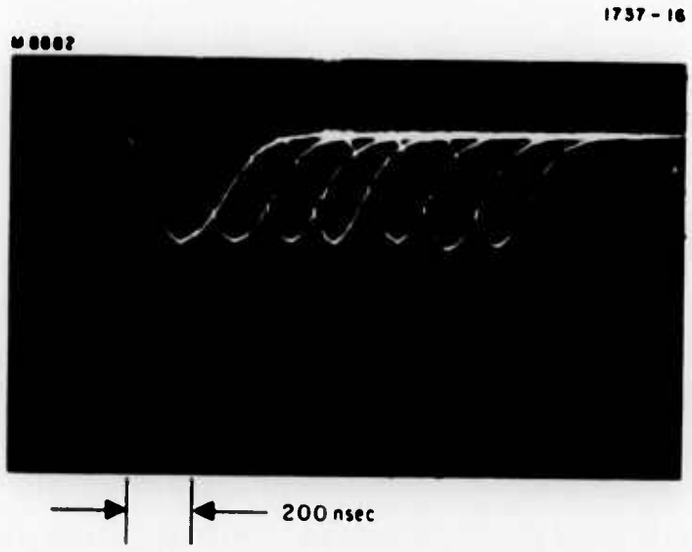

Fig. 13.
Oscilloscope Traces Showing Output of Low-Power Nd:YAG Laser for Seven Consecutive Shots.

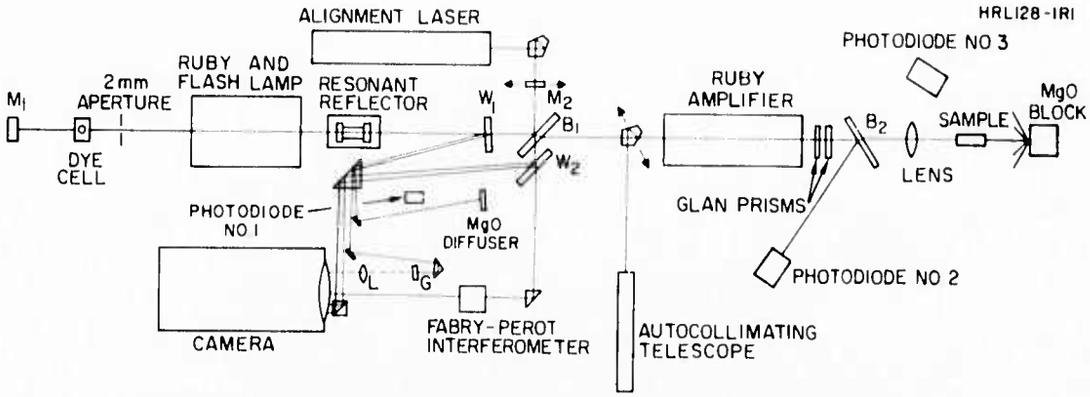

Fig. 14. Experimental Setup for Damage Experiments Using Single Mode Rube Laser and Amplifier.

HRL 265-5

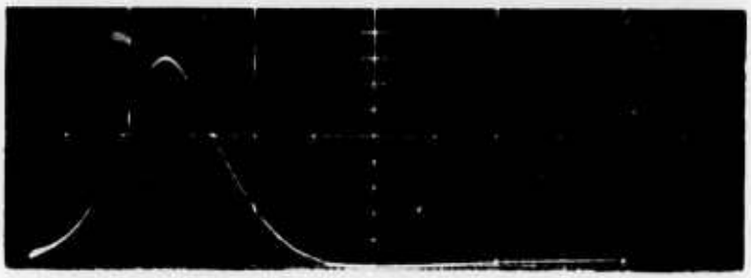

Fig. 15.
Oscilloscope Trace Showing Ruby Laser Output. Sweep Rate is 20 nsec/div.

TABLE IV

Characteristics of Lasers Used on Program

Properties	High Power Nd:YAG	Low Power Nd:YAG	High Power Ruby Laser
Wavelength	1.06 μm	1.06 μm	0.694 μm
Operating Characteristics	Single shot to 10 pps	Single shot to 50,000 pps or cw	Single shot
Mode Properties	TEM_{00}	TEM_{00}	TEM_{00}
Peak Power (Pulsed Mode)	300 kW	1 kW	~1MW
Energy per Pulse	~6 mJ	~0.25 mJ	~15 mJ
Pulse Width (FWHM)	18.5 nsec	250-300 nsec	~20 nsec
Av Single Mode CW Power	- -	1.5 W	- -
Measured Beam Radius[a] at Lens Focus for Damage Experiments	86 μm	37 μm	56 μm
Focal Length of Lenses Used in Damage Experiments	11 cm	11 cm	19 cm

[a] The beam radius is defined here as the 1/e radius for the electric field, which corresponds to the $1/e^2$ radius for the intensity.

T606

with power supply capable of delivering 8 kJ in a 3-msec pulse. The power supply employs a pulse shaping network of 20 sections, each section pumping for 150 μsec. The maximum gain obtained with the amplifier is about 10 dB.

Table IV compares the characteristics of the three lasers utilized for this program.

E. BEAM DIAGNOSTICS AND POWER CALIBRATIONS

1. Beam Diagnostics at 1.06 μm

Details of the beam spot sizes were determined by measuring the diameter of burn spots on unexposed developed Polaroid film for

known incident powers ranging from the burn threshold to the maximum power available from the laser. The measurements were made for the two Nd:YAG lasers employed in this program. For the Nd:YAG lasers, spot size was determined at the position of the entrance surface of the proustite samples that were studied. This position is slightly upstream from the waist of the beam as it is focused by the 11-cm lens.

For each laser, about 40 shots were taken for which burn spots were measured. The diameters of the burn spots were measured using an optical microscope with a calibrated reticle at 200 x magnification. The technique was found to be surprisingly well-suited to this sort of measurement. It was found that the burn spots are extremely well defined: the boundary between the burned and unburned regions of the film is very sharp. Examples of burn spots are shown in Fig. 16. The validity of this technique is based on the assumption that the film possesses a sharp burn threshold, and that the diameter of a given burn spot is equal to the beam diameter at which the intensity (or energy density) equals the burn threshold.

The following expression would then apply for a gaussian beam:

$$I_t = I_o \exp (- d_t^2/4a^2) \qquad (1)$$

where I_o is the peak intensity, I_t is the intensity at burn threshold, d_t is the diameter of the burn spot, and a is the characteristic 1/e radius for the intensity.

Taking logarithms we have:

$$\ln I_o = d^2/4a^2 + \ln I_t \qquad (2)$$

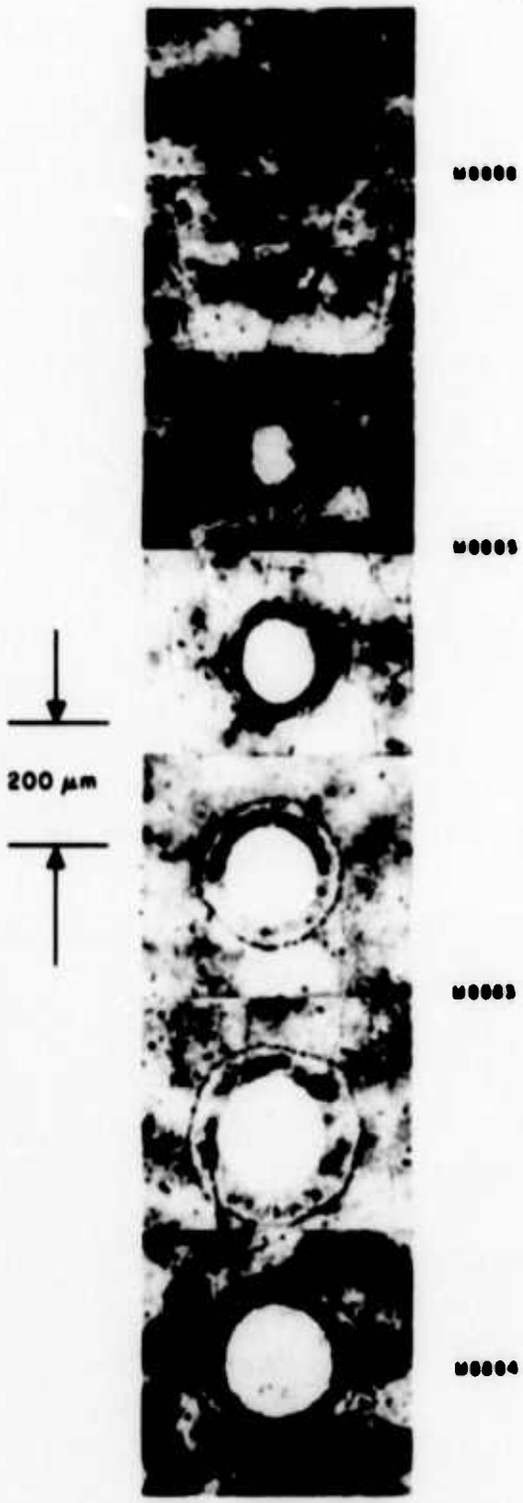

Fig. 16.
Photomicrographs of Nd:YAG Laser Burn Spots on Polaroid Film for Different Incident Powers.

From eq. (2) we see that a semilog plot of peak power versus the square of the burn spot diameter should give a straight line with slope equal to $1/4a^2$ and intercept equal to $\ell n\ I_t$ for a gaussian beam profile. Deviations from gaussian behavior will be evidenced as curvature in these plots. Data for the two Nd:YAG lasers are plotted in Figs. 17 and 18. Deviations from linearity are evident at the high-power end of these plots (corresponding to the wings of the distribution), and the curvature is such that the actual beam profile contains more energy in the wings than an ideal gaussian distribution. That is, the burn spots formed at high powers are larger than those expected for gaussian beams.

From the slopes in Figs. 17 and 18, we obtain values for a, the 1/e radius for the intensity of 60.8 μm for the high-power laser (Fig. 17) and 26.4 μm for the low-power laser (Fig. 18). The corresponding values for $\alpha = \sqrt{2}a$, the 1/e radius for the field (which is the $1/e^2$ radius for the intensity) are 86.0 μm for the high power laser and 37.3 μm for the low-power laser. The experimental accuracy for the spot size measurements is ±8%.

2. Beam Diagnostics at 6943 Å

A detailed series of beam profile and spot size measurements on the single-pulse ruby laser have been carried out in connection with another program.[6] The beam was photographed using a multiple exposure camera incorporating nine lenses, each one having a different amount of optical attenuation. Hence, each photograph contains nine different exposures of the same spot. By taking densitometer scans of the different spots, detailed information can be obtained about the spatial beam profile without requiring knowledge of the film response characteristics.[20] The results of a series of beam profile measurements are included in Reference (6). The far-field spatial profile was found to be gaussian down to 8% of the

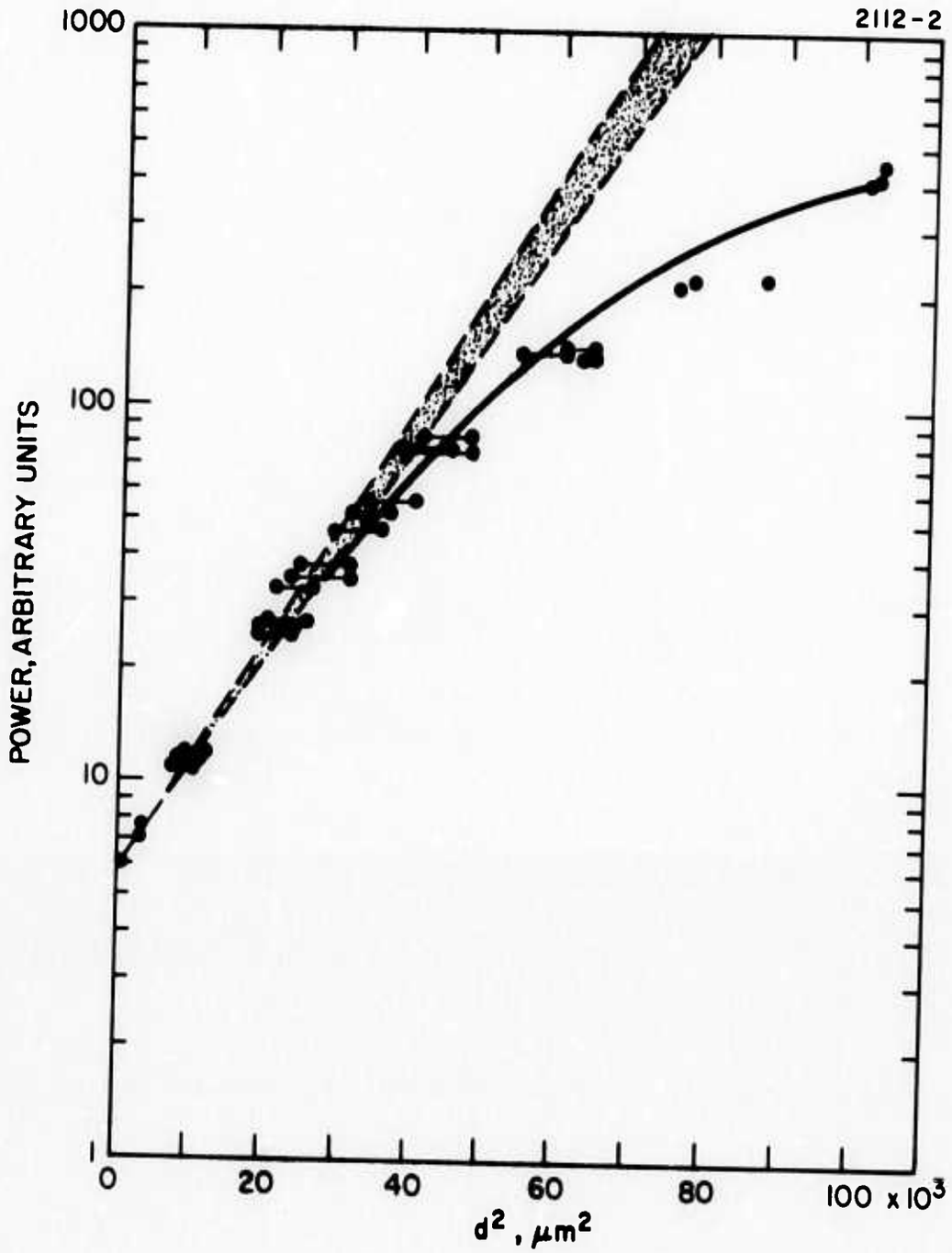

Fig. 17. Log P Versus d^2 for Burn Spots Taken at Focus for High-Power Nd:YAG Laser.

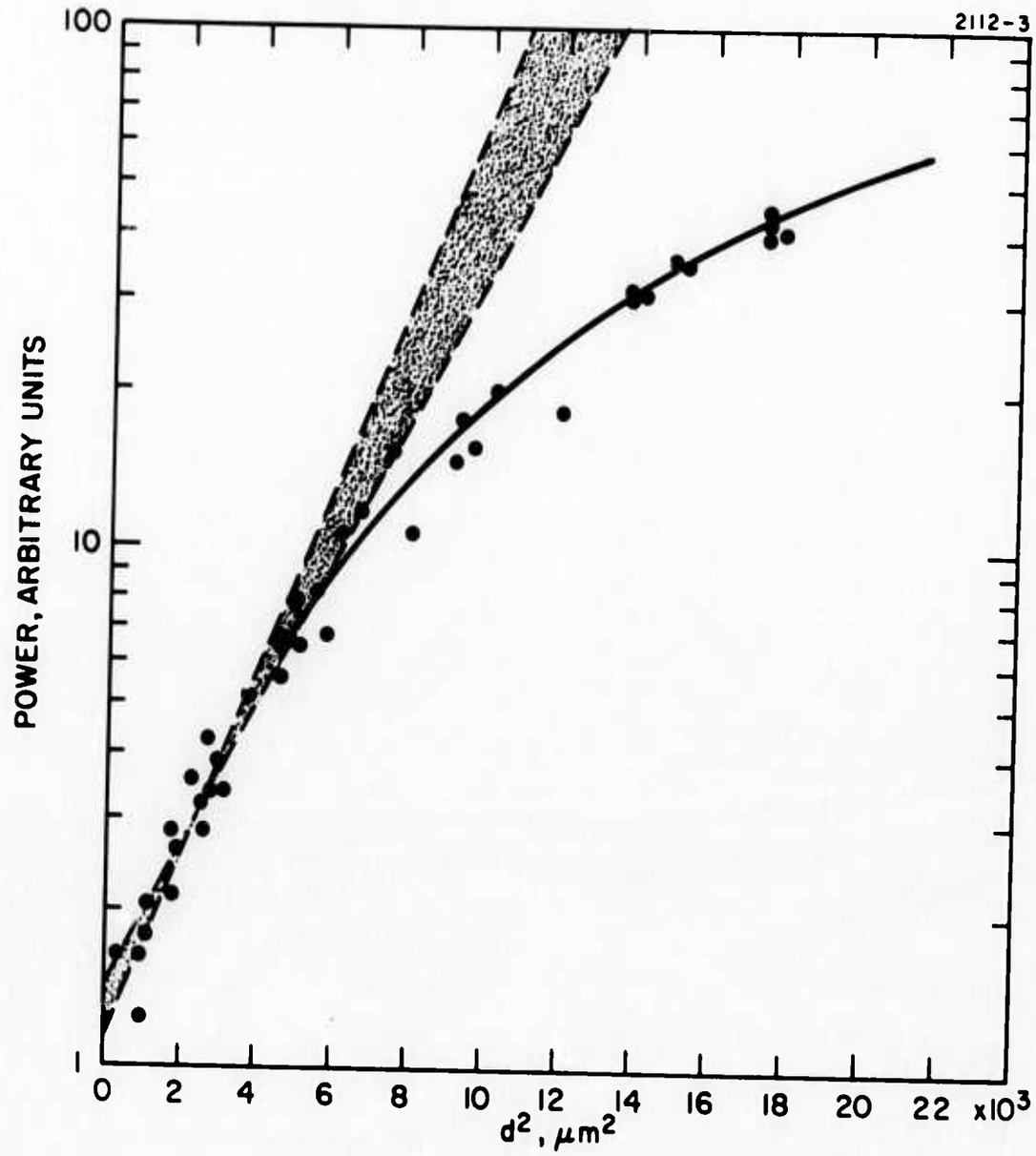

Fig. 18. Log P Versus d^2 for Burn Spots Taken at Focus for Low-Power Nd:YAG Laser.

peak. The spot size at the beam waist under the focusing conditions (19 cm lens) for the experiments carried out in this program for the pulsed ruby laser is 56-μm radius at the 1/e points for the electric field.

3. Power Calibration Measurements

For the pulsed ruby and high-power pulsed Nd:YAG lasers, the output energy was measured using a calibrated Hadron thermopile and simultaneously comparing the measured energy with the output of the monitoring Si photodetectors. From that point, the Si photodiodes were used as secondary standards. The energy of a single pulse was measured with the ruby laser while the total energy in a series of ten pulses was typically measured for the Nd:YAG laser operating at 10 pps. The energy per pulse was then obtained by dividing the total energy by the number of pulses. Temporal peak powers quoted in this report are obtained by dividing the total energy per pulse by the pulsewidth (FWHM). Power calibrations for the low-power Nd:YAG laser were carried out by measuring the average power in the beam using a CRL Model 201 power meter, while the laser was operating at a given known pulse repetition rate and simultaneously monitoring the output of the photodetector monitor. Hence, from a knowledge of the repetition rate, average power, and pulsewidth, values of peak power and energy per pulse can be obtained.

SECTION III

PLANS FOR NEXT PERIOD

During the next period, we shall pursue the possibility of providing a better quality surface finish on proustite than is obtainable by conventional abrasive polishing techniques. We have been experimenting with immersive polishing techniques for obtaining a "super polish" on sapphire with some success, but the apparatus needs to be further refined. When a super polished sapphire becomes available, its damage threshold will be compared with that of ion beam polished samples. We shall pursue further the behavior noted in Section C-2 for sapphire in an attempt to gain a better understanding of the temporal pulse shape of the transmitted pulse. In addition, we shall examine the temporal shape of the pulse reflected back from the sample surface during damage formation and attempt to correlate the temporal features of transmitted and reflected pulses. If it is possible to obtain a better quality proustite surface than that previously available, we will apply a low-reflectivity sapphire coating and again compare damage thresholds with the uncoated sample.

REFERENCES

1. C.R. Giuliano, "Laser-Induced Damage to Transparent Dielectric Materials," Appl. Phys. Letters 5, 137-139 (1964).

2. Damage in Laser Glass, American Society for Testing and Materials Technical Publication No. 469, edited by A. Glass, A. Guenther, C. Stickely, and J. Myers (American Society for Testing and Materials, Philadelphia, Pa., 1969).

3. Damage in Laser Materials, edited by A. J. Glass and A. H. Guenther, U.S. National Bureau of Standards Special Publication No. 341 (U.S. GPO, Washington, D.C. 1970).

4. Damage in Laser Materials, edited by A. J. Glass and A. H Guenther, U.S. National Bureau of Standards Special Publication No. 356 (U.S. GPO, Washington, D.C., 1971).

5. Laser Induced Damage in Optical Materials: 1972, edited by A. J. Glass and A. H. Guenther, U.S. National Bureau of Standards Special Publication No. 372 (U.S. GPO, Washington, D.C., 1972).

6. C.R. Giuliano, D.F. DuBois, R.W. Hellwarth, L.D. Hess, and G.R. Rickel, "Damage Threshold Studies in Laser Crystals," Final Technical Report, Contract No. F19628-69-C-0277, ARPA Order No. 1434, (September 1972).

7. C. R. Giuliano and D. Y. Tseng, "Laser Induced Damage to Nonlinear Optical Materials," Final Report, Contract No. F33615-71-C-1715, (September 1972).

8. C. R. Giuliano and L. D. Hess, "Damage Threshold Studies in Ruby and Sapphire," National Bureau of Standards Special Publication 341, U.S. GPO, Washington, D.C. (Dec. 1970) p. 76 (ed. by A. J. Glass and A. H. Guenther).

9. R. W. Hellwarth, "Role of Photo-Electrons in Optical Damage," National Bureau of Standards Special Publication 341, U.S.GPO, Washington, D.C. (Dec. 1970) p. 67 (ed. by A. J. Glass and A. H. Guenther).

10. C.R. Giuliano, "Time Evolution of Damage Tracks in Sapphire and Ruby," National Bureau of Standards Special Publication 356, U.S.GPO, Washington, D.C. (Nov. 1971) p. 44 (ed. by A.J. Glass and A.H. Guenther.

11. C. R. Giuliano and J. H. Marburger, "Observations of Moving Self-Foci in Sapphire," Phys. Rev. Letters 27, 905 (1971).

12. C.R. Giuliano, "Laser-Induced Damage in Transparent Dielectrics: Ion Beam Polishing as a Means of Increasing Surface Damage Thresholds," Appl. Phys. Letters 21, 39 (1972).

13. C. R. Giuliano, J. H. Marburger, and A. Yariv, "Enhancement of Self-Focusing Threshold in Sapphire with Elliptical Beams," Appl. Phys. Letters 21, 58 (1972).

14. C. R. Giuliano, "Laser-Induced Damage in Transparent Dielectrics: The Relationship between Surface Damage and Surface Plasmas," IEEE-J. Quantum Electronics 8, 749 (1972).

15. R. W. Hellwarth, "Fundamental Absorption Mechanisms in High Power Laser Window Materials," National Bureau of Standards Special Publication 372 (U.S.GPO, Washington, D.C., 1972) p. 165 (edited by A. J. Glass and A. H. Guenther).

16. C. R. Giuliano, "The Relation Between Surface Damage and Surface Plasma Formation," (Same as Ref. 15, p. 46).

17. C. R. Giuliano, "Ion Beam Polishing as a Means of Increasing Surface Damage Thresholds in Sapphire," (Same as Ref. 15, p. 55).

18. D. C. Hanna, B. Luther-Davies, H. N. Rutt, R.C. Smith, and C. R. Stanley, "Q-Switched Laser Damage of Infrared Nonlinear Materials," IEEE-J. Quantum Electronics QE8, 317 (1972).

19. N. Bloembergen, to be published.

20. I. M. Winer, "A Self-Calibrating Technique Measuring Laser Beam Intensity Distributions," Applied Optics, 5, 1437 (1966).